NASA/TM—2007-215025 AIAA–2007–4700

Lunar South Pole Illumination: Review, Reassessment, and Power System Implications

James Fincannon
Glenn Research Center, Cleveland, Ohio

November 2007

NASA STI Program . . . in Profile

Since its founding, NASA has been dedicated to the advancement of aeronautics and space science. The NASA Scientific and Technical Information (STI) program plays a key part in helping NASA maintain this important role.

The NASA STI Program operates under the auspices of the Agency Chief Information Officer. It collects, organizes, provides for archiving, and disseminates NASA's STI. The NASA STI program provides access to the NASA Aeronautics and Space Database and its public interface, the NASA Technical Reports Server, thus providing one of the largest collections of aeronautical and space science STI in the world. Results are published in both non-NASA channels and by NASA in the NASA STI Report Series, which includes the following report types:

- TECHNICAL PUBLICATION. Reports of completed research or a major significant phase of research that present the results of NASA programs and include extensive data or theoretical analysis. Includes compilations of significant scientific and technical data and information deemed to be of continuing reference value. NASA counterpart of peer-reviewed formal professional papers but has less stringent limitations on manuscript length and extent of graphic presentations.

- TECHNICAL MEMORANDUM. Scientific and technical findings that are preliminary or of specialized interest, e.g., quick release reports, working papers, and bibliographies that contain minimal annotation. Does not contain extensive analysis.

- CONTRACTOR REPORT. Scientific and technical findings by NASA-sponsored contractors and grantees.

- CONFERENCE PUBLICATION. Collected papers from scientific and technical conferences, symposia, seminars, or other meetings sponsored or cosponsored by NASA.

- SPECIAL PUBLICATION. Scientific, technical, or historical information from NASA programs, projects, and missions, often concerned with subjects having substantial public interest.

- TECHNICAL TRANSLATION. English-language translations of foreign scientific and technical material pertinent to NASA's mission.

Specialized services also include creating custom thesauri, building customized databases, organizing and publishing research results.

For more information about the NASA STI program, see the following:

- Access the NASA STI program home page at *http://www.sti.nasa.gov*

- E-mail your question via the Internet to *help@sti.nasa.gov*

- Fax your question to the NASA STI Help Desk at 301–621–0134

- Telephone the NASA STI Help Desk at 301–621–0390

- Write to:
  NASA Center for AeroSpace Information (CASI)
  7115 Standard Drive
  Hanover, MD 21076–1320

NASA/TM—2007-215025 AIAA–2007–4700

Lunar South Pole Illumination: Review, Reassessment, and Power System Implications

James Fincannon
Glenn Research Center, Cleveland, Ohio

Prepared for the
Fifth International Energy Conversion Engineering Conference and Exhibit (IECEC)
sponsored by the American Institute of Aeronautics and Astronautics
St. Louis, Missouri, June 25–27, 2007

National Aeronautics and
Space Administration

Glenn Research Center
Cleveland, Ohio 44135

November 2007

Acknowledgments

The author would like to thank A.C. Cook, M. Kruijff, J.L. Margot, D.B.J. Bussey, M.R. Rosiek, B. Archinal, and P.D. Spudis for their valuable insights, information, and assistance.

Level of Review: This material has been technically reviewed by technical management.

Available from

NASA Center for Aerospace Information
7115 Standard Drive
Hanover, MD 21076–1320

National Technical Information Service
5285 Port Royal Road
Springfield, VA 22161

Available electronically at http://gltrs.grc.nasa.gov

Lunar South Pole Illumination: Review, Reassessment, and Power System Implications

James Fincannon
National Aeronautics and Space Administration
Glenn Research Center
Cleveland, Ohio 44135

Abstract

This paper reviews past analyses and research related to lunar south pole illumination and presents results of independent illumination analyses using an analytical tool and a radar digital elevation model. The analysis tool enables assessment at most locations near the lunar poles for any time and any year. Average illumination fraction, energy storage duration, solar/horizon terrain elevation profiles and illumination fraction profiles are presented for various highly illuminated sites which have been identified for manned or unmanned operations. The format of the data can be used by power system designers to develop mass optimized solar and energy storage systems. Data are presented for the worse case lunar day (a critical power planning bottleneck) as well as three lunar days during lunar south pole winter. The main site under consideration by present lunar mission planners (on the Crater Shackleton rim) is shown to have, for the worse case lunar day, a 0.71 average illumination fraction and 73 to 117 hours required for energy storage (depending on power system type). The illumination at this site for each lunar day during a year varies dramatically, with as many as seven lunar days with negligible shadowing (i.e., maximal illumination/very little energy storage required). The maximum duration shadowing period for this site is primarily due to distant high terrain in the Malapert Mountain region (from 84 to 86 S, -10 to +45 E). Two potential sites with higher average illumination fraction and lower energy storage hours than the Shackleton site are shown to possibly have erroneously high site heights. In addition, a site at the Malapert Mountain peak counter-intuitively had a much lower average illumination fraction and much higher energy storage hour range, due primarily to nearby mountainous high terrain. This paper shows that by increasing the Shackleton site height by 100 m using a tower reduces the number of energy storage hours by 15 to 21 percent, although whether this is a mass optimized solution for a power system awaits further analysis. Completely eliminating energy storage through the use of practical tower heights does not appear feasible due to the nature of the shadowing terrain. Linking the Shackleton site with one ~10 km away was shown to improve the average illumination fraction from 0.71 to 0.84 and reduce the energy storage hours from 117 to 68 hours. Again, this may not be a mass optimum power system solution due to either heavy power beaming equipment or power cables (compared with simply increasing the energy storage size at the site). Linking other sites and including towers at both sites are shown to not completely eliminate the need for energy storage.

Introduction

The lunar south pole offers numerous reasons for space mission planners and designers to consider the location for unmanned and manned spacecraft deployments (e.g., robotic landers and rovers, short-term and long-term manned bases). Apart from scientific research and anticipated in situ material resources, a critical reason for deployment at the lunar south pole is favorable thermal and solar energy conditions at specific highly illuminated locations. Most spacecraft deployed to lunar sites require power provided by solar power generation and energy storage (either batteries or fuel cell type systems). Most unobstructed locations on the Moon's surface can be characterized by about 15 days of illumination followed by 15 days of darkness. However, near the poles, it is possible, due to terrain heights and Sun elevation angles, to have greater than 15 days of illumination with a subdivided illumination-darkness

period (due to high, shadow-casting terrain at various distances from the deployment site). Also, while an increased fraction of the time illuminated is clearly beneficial, more illumination-darkness subdivisions are even more valuable since they reduce the maximum shadow time which, in turn, reduces the deployed power system mass (especially for the energy storage). Thus, long periods of illumination and shorter periods of darkness enable smaller, lighter, more mission enhancing power systems.

It is critical in designing a solar power system for continuous operation to understand the worse case illumination conditions. Quantification of the illumination characteristics of various key potential deployment locations has uses beyond optimized power system design and sizing. Such data may be used for thermal design or for operational planning of power and thermal systems. Also, it plays a roles in operationally-related human functionality since the illumination-darkness cycling would appear somewhat random, varying dramatically through the year, with illumination nearly continuous during a number of months and highly variable for the remaining months. This is quite different from the 92 minute orbit period of the ISS or Space Shuttle which have a gradually changing darkness period from 0 to 36 minutes.

This paper reviews past illumination analyses and research for the lunar poles. The benefits, limitations and applicability of these analyses are discussed. Analyses generated by the author using digital elevation models (DEMs) and simulation software are presented to characterize lunar south pole illumination in a format useful in determining the optimum power system design and sizing.

Past Work

This section documents and reviews various analyses and prior work performed by researchers in this field. The various lunar polar sites discussed below are depicted in figure 1.

Past Work: Imagery Analysis

In one of the earliest analyses (ref. 1), Spudis, et al. used an imagery analysis method on images taken on Clementine Lunar Day 2 (the second month of Clementine imagery, 3/27/94-4/26/94) to create an animated set of overlays which, when quantified, indicated that the average illumination for Site A1 was >90 percent with a total of 50 to 60 hours of shadow and an annual average illumination of 95 percent. Bussey, et al. (ref. 2) subsequently documented an illumination analysis for the same lunar day and lunar region. An animation of the successive overlaid images was created (with a maximum spatial error of up to 1 km and an average of 500 m) which was digitized and pixel data collated. The intensity levels of the pixels was not assessed (i.e., partial illumination ignored, pixels beyond a set threshold were considered illuminated). Image gaps were shown for Lunar Day 2 (180 hours out of 708 hours in a lunar day). They assumed that any gaps due to these missing images as well as between successive imaging passes (10 hours) were the average of the preceding and following image. They stated that the images for Lunar Day 2 “were collected during wintertime at the south pole so the areas of darkness are at their maximum extent”. Bussey, et al. Lunar Day 2 results (refs. 2 to 9) may be summarized as follows: (1) Site A1 has >80 percent average illumination, (2) Sites B and C have >70 percent average illumination, (3) average illumination maps were created for the north pole/summer season (high illumination period) and the south pole/winter season (low illumination period), (4) illumination profiles as a function of solar sublongitude for Sites A1, B and C were presented, and (5) the illumination profiles showed a maximum continuous shadow period of 50 hours for Site A1, 188 hours for Site B and 140 hours for Site C. Reference 10, in results that seem to apply to Lunar Day 1 (at about one lunar day after the maximum darkness lunation, the first month of Clementine imagery was from 2/26/94-3/27/94), stated that one area has >70 percent average illumination and three areas have >50 percent during “maximum darkness”.

The most useful products of these analyses were the average illumination maps and illumination profiles. The former may be used for site selection while the latter may be used as a guide to quantifying the maximum shadow periods. However, in order to properly use these products, their limitations must be understood. First, there were imagery data gaps due to both orbital imaging pass intervals and technical

imagery problems. Due to the rapid changing illumination environment (the result of shallow solar angles and mountainous terrain), the potential for a great deal of change to occur in the interval between the imagery end points existed. This was especially a problem during large 'missing' image gaps. Second, illumination analysis data for the worse case lunar day was not available because Clementine imaging was not performed during that time. Even though Lunar Day 1 was not the worse case lunar day, it was significantly closer than Lunar Day 2, yet Lunar Day 2 data was primarily (perhaps exclusively) reported for the image analyses. It was stated in reference 2 that Lunar Day 1 had fewer images and less coverage than Lunar Day 2. However, at least for the Crater Shackleton area, an inspection of imagery shows a 'sufficient' number of images. There was less areal coverage due to the closer imaging altitude for Lunar Day 1 images; however, this proximity resulted in better resolution images. For solar power system design, the worse case lunar day needs to be considered, not higher illumination lunar days such as Lunar Day 2. Third, partial illumination was ignored in the image analysis. Because of partial blockage by the horizon terrain, reduced illumination of the Sun is possible and plays a role in conservative illumination quantification. If the image analysis of very partially lit pixels (a largely blocked Sun) indicates "full" illumination, this data cannot be used to conservatively size a power system because it is not adequately quantified. Fourth, the effect of the shallow sun angles on illuminating the terrain may result in terrain that appears dark but which actually has solar energy coming at an angle nearly tangent to the site. This means that a solar array pointing at the Sun would be able to be illuminated while the surface from which it is deployed may not be illuminated. Finally, the resolution of the imagery (470 by 470 m pixel size for Lunar Day 2) impacts a detailed site analysis since at a coarse enough resolution, the shadows induced by small terrain become washed out by albedo and reflections and shadow inducing small peaks and boulders may not be apparent.

Kruijff, et al. (refs. 11 and 12) documented an imagery analysis similar to that described by Bussey, et al. (ref. 2) although more detailed overlay information as well as average illumination data for both Lunar Day 1 and Lunar Day 2 of Clementine south polar imagery was presented. They described using software to rotate, re-size, and scale the images. The images were printed out and manually overlayed on an Aricebo radar image of the area. They composed an animation using this method for each lunar day. They described reflectivity models/algorithms and the creation of a wax model of the south pole region based on the Arecibo radar image and spotlights (a DEM was derived by scanning this model). Data regarding pixel intensity versus solar sublongitude (a useful way of depicting illumination and possible trends regarding the lunar surface) were presented for two of the key sites for both months. One such profile matches closely the illumination profile illustrated by Bussey, et al. (refs. 2 and 7). For Site A1, the average illumination was determined to be 91 percent for Lunar Day 2 and 71 percent for Lunar Day 1. Site A2 was determined to have 67 percent average illumination for Lunar Day 1. Site B was estimated to have with 72 and 91 percent average illumination for Lunar Day 1 and 2, respectively.

The main benefits of this analysis were to confirm some of the results of reference 2 and provide useful Lunar Day 1 average illumination data. Limitations are similar to those previously mentioned using imagery analysis. There were technically-missing (and/or analytically-omitted) images for both lunar days, especially during high shadow casting solar sublongitudes (from near ±20°). These gaps were assumed to have "interpolated values" which may introduce large inaccuracies. Also apparent was a problem with the pixel intensity method in that it is hard to determine the cause of the intensity variation; surface slope or partial Sun blocking by terrain. A lunar terrain surface parallel to the Sun's rays would likely appear dark but a fully Sun-tracking solar array deployed at that location would be illuminated. As with the reference 2 analyses, the worse case lunar day could not be assessed due to lack of Clementine imagery during that time frame.

Past Work: Digital Elevation Models

Margot, et al. (refs. 13 and 14) described the methodology used to create a DEM of the lunar north and south pole regions based on data gathered from the Goldstone Solar System radar of the Deep Space Network in 1997. Such a DEM could be obtained from a terrestrial site because the Moon's inclination is

6.7° with respect to its orbit plane about Earth, meaning that with optimum timing the terrestrial radar beam can be up to 6.7° above the lunar polar horizon. The radar covered each polar region of approximately 300 by 1000 km area. Examination of the radar data showed that the elevation range of the lunar south pole is 2.5 times that of the north pole region. They utilized ray tracing of the DEM to determine potential permanently dark regions through the year.

Based on the instrumentation and processing techniques, the height error for the radar DEM was stated to be ±50m. This should be considered the error for a completely flat region. However, for mountainous terrain or any variation from flat terrain, the actual error may be much more. The reason for this larger possible error is that the raw radar data was at a spatial resolution of 150 by 150 m, but in order to reduce height data noise, the data was averaged over a 600 by 600 m region. Within the 4 by 4 array of 150 by 150 m pixel heights, the possible range of heights (or deviations from the average) varies over the entire lunar surface depending primarily on topography. Added to this is the problem of blank radar data for terrain pixels due to blockage of the radar beam by lunar terrain. The algorithm for averaging these data are such that blank radar data are not included in the height average and >25 percent blank heights result in a null height for a 600 by 600 m DEM pixel. Non-flat terrain height error can only be quantified or bounded using the raw height dataset (only available from the dataset author).

Of particular interest to understanding the radar DEM was a discussion of how the model was validated and corrected. Validation of the height model was based on Clementine laser altimetry data which was assumed to be the reference (with a 150 m radial error in height). A 100 m RMS deviation between the laser data and radar DEM for 70 to 80° latitude existed and a correction applied of 0.07 and 0.1° to the north and south pole DEM respectively in order to better match the laser points. This was termed a “small residual slope” in the radar data and occurred mostly along the range direction. The origin of these slopes was unknown. For the poles, since the laser data are along one edge of the radar DEM, the absolute height errors could become “as large as the product of the slope and the range extent (i.e., 200 m)”.

References 15 to 19 documented the derivation of DEMs using stereo analysis of Clementine imagery. There are two DEMs that have been generated using this method. The first DEM (refs. 15 and 16) (by Rosiek, et al.) is associated with the USGS (http://astrogeology.usgs.gov/Teams/Geomatics/photogrammetry/topography_lunar.html). This model omits a small and critical region near the lunar south polar region (surrounding and including Crater Shackleton). In addition, this DEM significantly smoothes the terrain heights. Compared with the radar DEM, this smoothing seems somewhat artificial. Both of these factors make it difficult to utilize the DEM to predict illumination near polar regions. The second DEM (refs. 17 to 19) (by Cook, et al.) is associated with the Smithsonian Institute Center for Earth and Planetary Studies. It includes the Shackleton region and does not perform the kind of terrain smoothing seen in the USGS DEM. The resolution of this DEM is 1 by 1 km and covers from 60 to 90° for both the lunar north and south pole. This DEM covers a much larger area than the radar DEM and covers areas that could not be seen by Earth based radar. The limitation of all stereo-derived DEMs is the number of steps needed to process the data which results in uncertainty, error, and “noise” (erroneous heights). Authors of all DEMs have utilized the Clementine lidar data (available down to -79° latitude) to assist in generating absolute heights for their models, even though the lidar data set required significant filtering to extract absolute heights. (For example, with the lidar continuously firing pulses, two data acquisitions may occur at nearly the same time. However, although one point is sent to the final, filtered dataset, comparing the two unfiltered points show they can differ from -14 to 17 km with an absolute average of 6 km.)

Past Work: Analysis Tools/Simulations

Reference 20 documented analyses performed using an analytical tool/simulation model which utilized the north and south polar radar DEMs to generate average illumination maps for both the worse and best case lunar days. They concluded that illumination simulations using the radar DEM were “in general agreement with Clementine photographic animations.” They presented only one illumination

profile (for a north pole location). They reported that the majority of the south polar regions spend more time in darkness than equatorial regions, even in summer. Sites A1, B, C were assessed as highly illuminated (>75 percent of the time) (previously identified in ref. 2). Site D was indicated a having the highest illumination on the south pole (75 to 95 percent average illumination). This site is reassessed later in the present paper.

Comparisons of south pole lunar imagery with the radar DEM simulated illumination were reported in reference 3. They performed "several simulations" using both the Clementine stereo-derived (i.e., Smithsonian version) DEM and the radar DEM. They found the radar DEM to be reasonably accurate and produced a more accurate replication of the shadow patterns seen in the Lunar Orbiter images and Clementine UVVIS frames than the other DEM.

Both of these papers provide an analyst with encouragement that it is useful and feasible to utilize the radar DEM for detailed illumination assessments. The former paper was valuable in that it depicted the average illumination map for the worse case lunar day, a useful correlation of the average illumination maps derived from imagery analysis.

Kruijff (ref. 21) described the algorithms and specific implementation of a lunar surface visibilities computer program. Visibilities to orbiting satellites, rovers and the Sun are assessable by the program. The program seems somewhat coupled to a particular DEM input created from a wax model of the south lunar pole, but could likely be adapted to other DEMs. Some of the methodologies and concepts described in the reference are useful in developing an independent model.

References 22 to 24 described analysis software used to predict illumination using the radar DEM of the lunar south pole for a particular lunar application. These references are somewhat less useful than the Kruijff work, however, have some interesting descriptions of methodologies.

Past Work: Malapert Region

Reference 25 presented a simplified illumination analysis of a site located at the peak of Malapert Mountain, a location which has a good visibility to the Earth and which has been claimed to have good illumination. The analysis assumed a perfectly spherical lunar surface (with no irregularities due to terrain) and a user specified site altitude. They summarized the illumination on a yearly basis (89 percent full illumination for the entire year and 4 percent added to this to account for partial illumination). This format is of little use for power system designers. Fortunately, the author also provided the monthly sun setting data to identify the critical energy bottleneck of worse case illumination lunar day. This period was specified to be 159 hours of full shadowing (78 percent average illumination) and 199 hours if partial shadowing is included (72 percent average illumination). This site is reassessed in the present paper.

Past Work: Landing Sites

A landing site analysis for the north and south pole was documented in reference 4 which shows an overlay of a 40- by 40-m-high resolution image (from ref. 9) with an illumination map (likely for Lunar Day 2). A 40- by 40-m-high resolution mosaic of Clementine south polar imagery was also used in reference 26 to identify good landing sites. No coordinates were provided for the sites, although the imagery pinpoints them. An overlaid illumination map is shown but is of unknown origin and of fairly generalized description.

Analysis Data Sources

The primary data sources used in the present illumination analysis are from Clementine imagery and radar data.

Analysis Data Sources: Imagery

Clementine spacecraft south polar imagery from two lunar days in 1994 was used in this paper for analysis comparison and validation. A good source for these images, associated image data, and an excellent search engine is at the French space agency's website (http://clementine.cnes.fr/index.en.html).

With regards to both imagery and analysis, this paper defines the key time periods as follows. The worse case lunar day is the time period in which the average solar elevation is a minimum for the lunar year (note that the worse case lunar day could possibly be different if based on some other metric). Since Clementine operated in 1994, then the worse case lunar day for that year occurred from 2/2/94-3/3/94. The solar elevation range for that period was from -1.74° to -1.31°. The first lunar day of Clementine south polar imagery (Lunar Day 1) occurred from 2/26/94 to 3/27/94, which was effectively after the worse case lunar day. The solar elevation range for this time period was from -1.67° to -1.23°. During that time, 63 useful images were collected of the near south pole area. The second month of imagery (Lunar Day 2) was from 3/27/94-4/26/94. The solar elevation range was from -1.34° to -0.68°. During that time, 62 useful images were collected of the south pole area. Some images were taken of the region during Lunar Day 3 (4/26/94-5/25/94). The solar elevation range was from -0.67 to 0.13°. The average altitude: image resolution for Lunar Day 1 was about 800 km: 200 by 200 m pixels and for Lunar Day 2 about 1800 km: 470 by 470 m pixels. Some high resolution images were also gathered at the poles at 40 by 40 m.

Lunar Orbiter imagery was examined for possible use in validation and comparison. Only a limited number of Lunar orbiter images covered the Crater Shackleton area of the lunar south pole. These were from Lunar Orbiter 4 (images 5, 6, 8, 9, 44, 58, 70, 82, 94, 106, 118, 130, 154, 166, and 179) which took place from 5/11/67 to 5/24/67 and one image from Lunar Orbiter 5 (image 21) taken on 8/6/67. The Lunar Orbiter 4 images covered a time period equal to two months prior to the worse case lunar day (which occurred in July 1967). The only image closer to the worse case lunar day was the one Lunar Orbiter 5 image. Because there were many more Clementine images closer to the worse case lunar day, it was decided that it was unnecessary to perform any validation comparisons using the Lunar Orbiter images.

Analysis Data Sources: Digital Elevation Models

The radar DEM used in this analysis is discussed in detail in reference 13. DEMs derived from the Clementine imagery (the USGS DEM (refs. 15 and 16) and the Smithsonian DEM (refs. 17 to 19)) were not utilized in this paper for reasons outlined in the section "Past Work: Digital Elevation Models".

Analysis Method

This section discusses the several ways to assess illumination of the lunar polar regions; imagery overlays, hard models, 3D computer models and analytical computer models.

Analysis Method: Imagery Overlays

The first method (used by the authors of refs. 2 and 11) overlays imagery of the area of interest and averages the brightness for each overlain pixel. This may be done using computers or transparencies. For Clementine images, it was necessary to scale, skew (due to off nadir pointing of the camera), remap (due to the curvature of the lunar surface), rotate, and translate the image for very accurate overlaying.

This method was utilized to assemble the Clementine images for the first two lunar days of its operation (Lunar Day 1 is shown in figs. 1 and 2). This image used the Photoshop "lighten" blending option to combine the images. A few orbits had inadequate features to permit overlay (due to high shadowing) and could effectively be considered totally shadowed for the region of interest. Skewing and remapping were omitted, although scaling, rotation, translation were performed. No contrast enhancement was performed on the imagery which permitted the examination of possible partial illumination and as-imaged pixel intensity values.

Analysis Method: Hard Model

The second method creates a hard model out of some sort of moldable substance (such as wax) which can be modified physically via trial and error to match a baseline image(s). Reference 11 used this approach to match a radar image of the south lunar pole (spotlights were used in place of the illuminating radar beam). A DEM was then derived from the scanned hard model.

Analysis Method: 3D Computer Model

The third method improves upon the second method by converting a DEM into a format that can be read by a 3D graphical modeler (used in refs. 3 and 14). Light positions representing the Sun may be created and the scene rendered using ray traced shadowing to create a graphical simulation of the illumination of a region. This method is useful for examining large numbers of pixels simultaneously and many Sun positions in a relatively short time. The user may adjust groups of polygons to obtain better matches when comparing with actual images. The results using this method are illustrated in figure 3.

Analysis Method: Analytical Computer Model

The fourth method uses an analytical tool to calculate the blockage of the Sun by terrain defined using a DEM. References 20 to 22 are examples of this work.

This was used as the primary method for quantitative analysis of lunar south pole illumination. A FORTRAN computer program was developed to perform this function. Existing algorithms (ref. 27) were used to calculate the solar azimuth and elevation. This data was successfully compared with analogous values from the JPL HORIZONS on-line ephemeris (http://ssd.jpl.nasa.gov/?horizons). The remaining algorithms were developed with general inspiration from preceding workers in this field. One such concept was the creation of a terrain elevation/azimuth "mask" representing the horizon as viewed from a particular site.

One algorithm converts the pixel (i.e., elemental area) data from the image file (which is the easy method used to store, edit and represent the DEM data) into altitude offset data for use in the geometry calculations. This conversion involves the use of spherical geometry (i.e., lunar surface curvature is accounted for), definition of the latitude/longitude projection of the DEM on the flat image file, usage of an average lunar radius (1737.4 km), addition and/or subtraction of any altitude offset to the site and/or surrounding terrain (to account for assumed height error and tower height).

The program goes through all the DEM height points and calculates the elevation of each terrain elemental area as viewed from a user specified site and stores the highest such elevation data in its specific discrete azimuth bin. After all the DEM pixels are examined, the program will have generated a topographic horizon elevation profile as a function of site azimuth. Elevation from a site is measured with a zero degree value representing the plane tangent to the site location normal (negative elevation is downward). Azimuth for a site is zero for a line toward the lunar north pole along the lunar surface. An azimuth of 90° East is obtained by going clockwise on the surface (looking downward at the site).

After the elevation-azimuth horizon profile is obtained for the site, the algorithm then compares the Sun location (solar azimuth/elevation) for the user specified time period with this profile. If the terrain elevation is lower than the Sun, there is illumination; if the terrain elevation is higher than the Sun elevation, then the terrain is shadowing the Sun. The special case of partial solar blockage by the terrain has been accommodated. The algorithm allows for a disk modeled Sun with 0.53° angular width. Whenever the terrain elevation is within the range of Sun elevation defining the solar disk, the area of blockage of the disk is calculated and the partial illumination calculated. This is technically only the horizontal partial blockage of Sun, there may also be a vertical component of the blockage. Calculation of vertical partial blockage was not implemented at this time.

Finally, the program generates output data in various formats such as maps of data for selected regions of interest, time changing illumination profiles and characteristic terrain/solar azimuth/elevation profiles for a site.

Potential High Illumination Sites

References 1 to 9 identified three sites of relatively high illumination near the lunar south pole during its winter season (i.e., Crater Shackleton rim, a connecting ridge from this rim, and Crater de Gerlauche rim). Using a similar imagery analysis method, refs. 11 to 12 assessed three sites (i.e., two on Shackleton rim and one on the connecting ridge). Using a radar DEM analysis, reference 20 assessed four sites (i.e., at the Crater Shackleton rim, the connecting ridge, the Crater de Gerlauche rim, and a Crater Sverdrup rim site). The peak of Malapert Mountain was assessed in reference 25 as a potentially high illumination site.

Figure 1 summarizes, in a Lunar Day 1 Clementine imagery overlay, the sites considered in this paper. Site locations were selected based primarily on the radar DEM heights and may not precisely match prior analysts' identified locations. The listed latitude and longitude locations are approximate (due to polar grid variations) and should only be used as a guide.

One Crater Shackleton rim site (Site A1, ~89.8S, ~213E, and ~1.9 km height) has been previously determined to have the most illumination at the south pole. An alternative to this site (in case Site A1 proves too rough or steep) is Site A2 (~89.9S, ~237E, and ~1.7 km height) or Site A3 (~89.9S, ~301E, and ~1.7 km height). The "connecting ridge" site (Site B, ~89.4S, ~233E, and ~1.9 km height) is the nearest non-Crater Shackleton rim site to Site A1 (13 km) and may potentially be energy- connectible. The Crater de Gerlauche rim's Earthward face has several points with high illumination of which Site C was selected for presentation in this paper based on having the highest height (~88.6S, ~293E, and ~2.1 km height). The Crater Sverdrup rim has one site (Site D, ~88.0S, ~195E, and ~3.2 km height) near that area's peak. A Malapert Mountain site (not shown: Site E, ~86S, ~4E, and ~4.8 km height) is located near the mountain's peak.

Other sites identified via DEM analysis include Site F (~88.9S, ~129E, and ~2.2 km height), Site G (~88.9S, ~258E, and ~3.1 km height), and Site H (~89.4S, ~121E, and ~1.5 km height). A number of other sites identified via radar DEM analysis relied too heavily on terrain outside the radar DEM available data and, thus, approximated by a uniform sphere, so were not considered in detail in this paper.

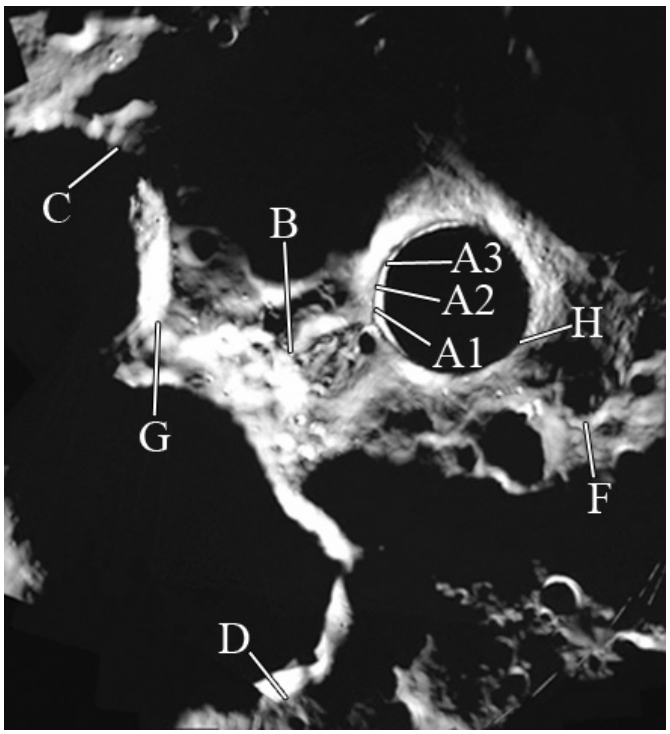

Figure 1.—Potential highly illuminated sites.

Metrics

Many of the previously published illumination analyses have referred to the "average illumination" over lunar days (or "lunations" or "month"). Such data are useful to identify potential high or low illumination locations, but have limited use for engineering applications such as power system design. In sizing a power system which uses solar power and a form of energy storage, the maximum duration of shadowed operation must be quantified. "Average illumination" does not describe whether the illumination is one continuous period or a large number of evenly dispersed periods. Each of these extremes may produce a very different mass optimum power system design (it is likely the illumination character is somewhere in between). For instance, at the lunar equator the average illumination is 50 percent (over one lunar day) and the cycle is about 15 days illuminated and 15 days in darkness, a rather long period for which to design energy storage. The same average illumination value at the poles could have much shorter cycles. For this reason, it is essential to have a time varying illumination fraction profile of candidate power system deployment sites. This profile data may be used in more detailed power system sizing computer programs (which consider system efficiencies, operational constraints and capabilities) to determine a mass optimized power system design.

In addition to the illumination profile, another useful metric that supersedes average illumination in importance is "energy storage hours". This method of defining the minimum number of hours for which the power system must be designed makes use of the illumination fraction profile to identify the maximum shadowed operation period. This is not merely the maximum continuously shadowed period. Because the illumination profile may have many brief shadow periods during which a power system must provide power and may have many brief illumination periods to recharge the energy storage system, the number of energy storage hours is highly dependent on the power system characteristics.

For a fixed energy storage 'container' size, a power system with oversized solar arrays and enhanced energy storage system (higher recharge rates) can recharge in shorter time than a power system with much smaller solar arrays and an energy storage system with lower recharge rates. For typical low Earth orbiting spacecraft, the power system can have up to 56 minutes to recharge the energy storage for 36 minutes of shadowed operation. One typically designs a mass optimized system such that the solar array is somewhat larger than it needs to be to simply provide user power during insolation in order to charge the energy storage over the insolation period to provide the same user power level during the shadowed period (i.e., eclipse). A solar array much larger could have the ability to recharge the energy storage much quicker (if the energy storage was capable of handling higher currents, etc.) but this capability is generally not needed in orbiting spacecraft. Conversely, a somewhat smaller solar array can be used but then lower eclipse power levels are required. This kind of load cycling is not frequently implemented. For a quasi-random appearing illumination profile on a lunar surface site, the determination of best solar array and energy storage size is more complicated. It may be justifiable to have oversized solar arrays since they weigh much less than energy storage, however, if the energy storage cannot handle the extra current provided by the solar arrays, it may be irrelevant. These are detailed design considerations that are outside the scope of this paper.

To summarize the range of hours that are likely to be required for the energy storage, it was decided to simplify the definition of energy generation-energy storage design into a term called "recharge ratio". This simplification was required since this analysis is not intended to perform power system sizing or design. A recharge ratio of 0.25 (.5, 1, 2 or 4) means that it takes 1/4 (1/2, 1, 2 or 4) recharge hour(s) to charge one discharged hour of energy storage. There are two ways to view this ratio. First, for a fixed user power level in both the illuminated and shadowed states, one can interpret a ratio of 0.25 as a power system with four times the generation capability enabling the recharge time to be reduced to a quarter of what would be normally required. Second, the ratio can be considered the user power level reduction during the shadowed period (e.g., a ratio of 0.25 means the shadowed period user power is reduced to one quarter the level during the illuminated period). The continuum of recharge ratios and how they relate to power systems is approximate. It is assumed that a ratio of 0.25 is near the "very fast recharge" end of the power system design continuum whereas a ratio of 4.0 is near the "very slow recharge" end of the

spectrum. Note that the low Earth orbit spacecraft example scales to approximately a 1.5 ratio, a very high Earth orbit spacecraft would be toward the 4.0 ratio and a power system at the lunar equator would most likely be near a 1.0 ratio.

When the preceding ratio is applied to the illumination fraction profile (as a function of time), then the cumulative total of energy storage hours charged/discharged can be tallied without having to consider system efficiencies, operating power levels, system limitations/characteristics. For every time step (i.e., one Earth hour intervals) of the profile when there is full illumination, the illumination is divided by the recharge ratio and this amount is added to the cumulative total. For partial illumination or no illumination, the power system is assumed to discharge to maintain the nominal operating power level which would normally occur when there is full illumination. In this case, the difference in illumination from 1.0 is subtracted from the recharge hour cumulative total. This process is repeated for the entire lunar day. When starting with a zero value in the cumulative total, the deficit over the lunar day would indicate the energy storage hours required for that case. Note that usually in energy storage designs some margin or excess is required for various reasons. None were added in this report.

Validation Work

In performing illumination analysis validation it is necessary to assembly a correctly registered (i.e., oriented, scaled) collection of actual imagery of the lunar pole near a time period of interest. Figure 2 shows four overlays of the lunar south pole region derived from the Lunar Day 1 Clementine imagery (the lunar day following the worse case lunar day) grouped according to solar sublongitude. Image A corresponds to a range of solar sublongitude from -45 to 45° (the Sun is near the same direction as the Earth facing side of the Moon). Image B is for the solar sublongitude range of 45 to 135° (the Sun is in the lunar East quadrant). Image C is for the solar sublongitude range of 135 to 225° (the Sun is on the lunar side which is not facing the Earth). Image D is for the solar sublongitude range of 225 to 315° (the Sun is in the lunar West quadrant). Images B and C show that the inner slope of Crater Shackleton (near the peak illumination sites) is highly illuminated, whereas for image A and D the outer slope is highly illuminated. The peak illumination site seems to lie on a ridge between the two slopes, but is very difficult to pinpoint due to the resolution of the images. (For illumination with the Sun nearly at zero elevation, it seems likely that the terrain shown in Clementine imagery would be dark if it is normal to the Sun angle.)

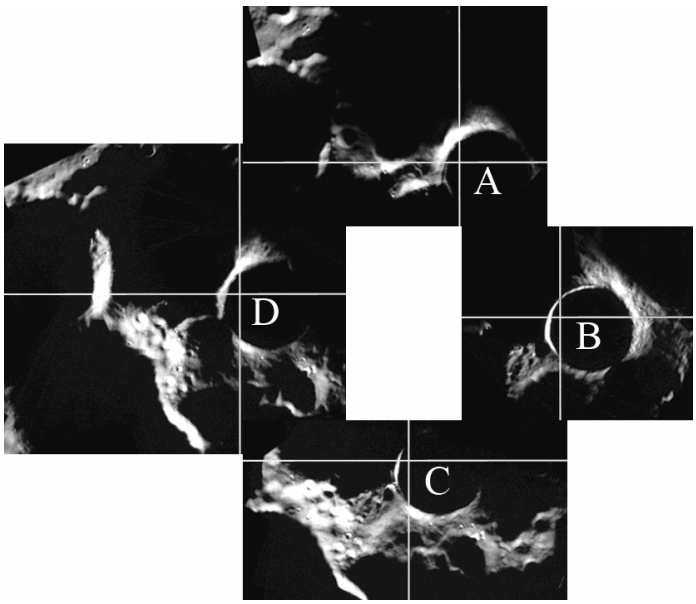

Figure 2.—Lunar Day 1 overlays grouped by solar sublongitude.

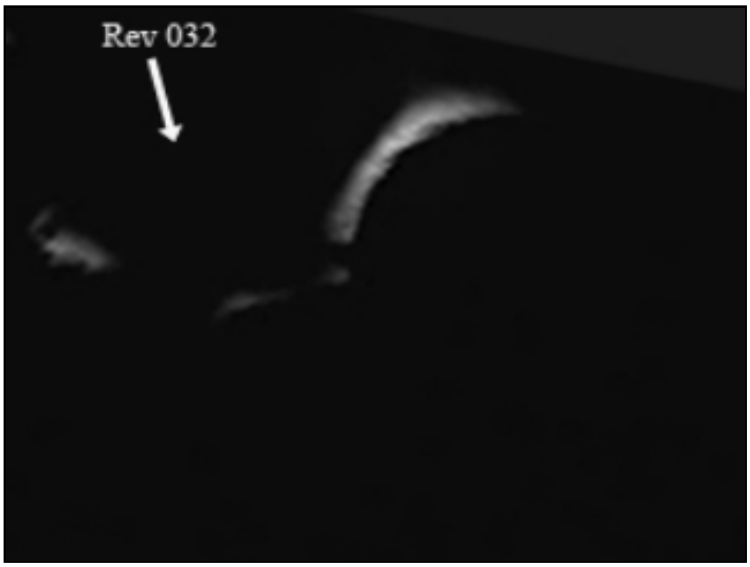

Play movie

(An animation of all existing, relevant Lunar Day 1 Clementine imagery is shown above (the video animation can be viewed within the .pdf file online at http://gltrs.grc.nasa.gov). Note that this animation shows the Clementine orbit number of the image and the direction of the Sun's rays. As noted by the orbit number, for animation continuity, some Lunar Day 2 images are shown where Lunar Day 1 images are not available. Also, some black images are due to complete shadowing of the Shackleton area.)

Examination of successive overlaid images shows some shadowing by "small features" on Crater Shackleton rim which seem to correspond to peaks that appear in the radar DEM. Also, this examination shows what appears to be partial Sun blockage (or, less likely, sloped terrain) that causes terrain to be generally dimmed from typical illumination levels.

To perform large area validation comparisons of images derived using the radar DEM and the Clementine images, a 3D computer rendering tool, 3DMAX, was used. The radar DEM was converted from its native format (a 2D representation of a part of a spherical surface in an image file format of grayscale values representing various altitudes from the mean lunar diameter) into a stereolithography format. Blank data regions were given extreme low heights.

Two limitations exist to the 3D rendering validation method. First, computer/software memory limitations allowed only three-vertexed polygons in which each of the vertexes is a center of adjacent elemental DEM areas. However, since each DEM elemental area is a four vertexed surface with a height value representing an average over the area, the three-vertexed polygons will not match the original data. Secondly, the highly sensitive nature of surface slope on the brightness of the pixels, make any comparisons somewhat suspect. The DEM, by its definition, provides a set of surfaces of which ALL are normal to the radius vector of the Moon, which does not match the reality of lunar terrain surfaces. Because the DEM provides average heights in each areal element and due to the complexity of the real terrain, any interpolation of surfaces to create valid slopes would likely be incorrect unless higher resolution elemental areas are obtained. Given these limitations, it was assumed that this method was adequate for approximate validation comparisons due to the large number of polygons at fairly random orientations of which a large number had a good chance of being illuminated (although the actual illumination amount may be incorrect).

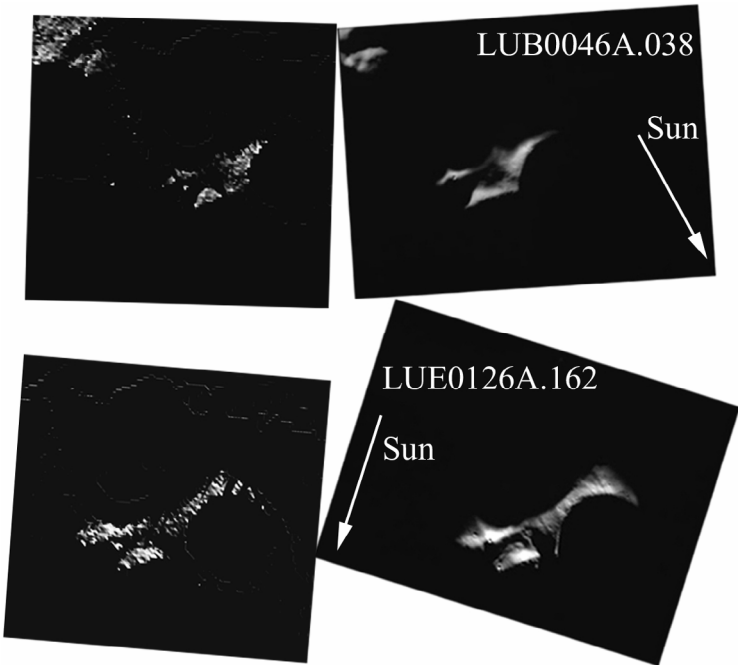

Figure 3.—Comparison of radar DEM simulation images with Clementine images.

Figure 3 shows example Lunar Day 1 illumination comparisons of radar DEM ray-traced simulations (on the left) and Clementine images (on the right). Orbit 38 is on the top and orbit 162 is on the bottom. Many other image comparisons were performed. General comparisons seemed qualitatively acceptable. The orbit 162 images show Crater Shackleton inner slope differences which make it less visible in the simulation image. Also, there appear to be more small illuminated areas, some of which may be due to the artificial slopes of the imported DEM data and some points are possibly due to erroneous DEM height data. One of these points in the upper left image is Site G which does not show up in the higher resolution image on the right. Some apparent pointed shadows in the left images are due to high, distant terrain and using a point light source in the rendering tool (incorporating an appropriate width light source would likely reduce such shadow striations).

Another approach to validation was to comparing imagery analysis illumination profiles for Site A1 Lunar Day 2 (those generated independently by Bussey, et al. (ref. 2) and Kruijff, et al. (ref. 12)) with results obtained using computer analysis of the radar DEM. Reference 2 identified shadow periods at solar sublongitudes of 233 to 253°, 274 to 284°, 359°, 36°, and 304°. Reference 12 presented a pixel intensity assessment with low brightness periods at 229 to 254°, 268 to 273°, 282 to 283°, 35°, and 304° (that reference had no images to assess from -10 to 20°). The radar DEM computer analysis results for illumination fractions below 0.2 (see fig. 5) showed the following shadow periods for Lunar Day 2: 238 to 246°, 266 to 267°, 356 to 360°, 37°, and 301°. Of course, figure 5 shows a number of other brief shadow periods that were not identified in the previously reported imagery analyses. This could be because the Clementine images did not coincide with the radar DEM analysis shadowing event timing (i.e., the event occurred in the 10 hour image gap or during a missing image gap). Other possibilities for differences include erroneous radar DEM areal element heights (some key outliers in height may actually be lower than in reality), the radar DEM may need some general correction to heights (a lowering of the region near the pole, or raising of the heights away from the pole in the radar DEM that would enhance the comparison), and/or a vertical partial illumination model of the Sun may be required. Whatever the reason for the relatively short duration differences, it is clear that because the illumination profile of reference 2 was assessed for Lunar Day 2, the maximum duration shadowing period that would be encountered during the worse case lunar day (from -6 to +53° solar sublongitude) was not apparent but, as described in a later section, drives the energy storage requirements for Site A1. The major difference for

Lunar Day 2 from the imagery analysis method and radar DEM analysis method is in the range from solar sublongitude 229 to 284°. Examination of individual images show that the shadowing onto Site A1 during this period is due to relatively near terrain (near Sites B and C) as opposed to distant terrain (possibly beyond the radar DEM coverage). General height adjustments that lowered the terrain heights near Site A1 improved the comparison for the period (as well as raising the terrain heights away from Site A1 generally or even in particular regions), however, no basis was found for such general adjustments. The drawback from lowering Site A1 terrain heights is that this would generally increase the shadowing of Site A1 for the rest of the solar sublongitudes as well. It is generally desirable to understand the cause or mechanism for applying such height correction factors prior to applying them.

Analysis Results

Illumination cycles for a site are fairly repetitive each year. The primary variation is the time phasing of the cycle which affects which lunar day has the worse and best case illumination. In this report, analyses are presented for 1994 since the Clementine spacecraft acquired relevant imagery during that year which can be used for comparison and validation purposes. The several distinct lunar days considered in this analysis, the worse case lunar day, Lunar Day 1, Lunar Day 2, and Lunar Day 3 have been defined above. For 2020, the worse case lunar day occurs in September of that year.

In all of the analysis figures that follow, the term elevation refers to the angle of the terrain at the horizon or the Sun as measured from the tangent plane to the site under consideration (i.e., not ‘elevation’ such as kilometers or meters in terms of height). The figures present the sun and terrain elevation and illumination fraction as a function of solar sublongitude even though the analysis software utilizes site azimuth in performing calculations and depicting results. A simple conversion is provided to assist the reader in using the data in the site azimuth format. The illumination fraction profile has high values meaning fully illuminated, low values being fully shadowed, and a linear variation in between representing partial illumination. These profiles permit the reader to simulate a visual panning from the site and enable one to visualize the horizon as well as the sun position relative to the horizon. The illumination fraction assumes the viewer (or solar array) is facing directly at the Sun. No reflected energy or albedo is included in this fraction. No shadowing due to locally deployed hardware (e.g., other solar arrays) or eclipses due to the Earth at the site (1-1.7 hours full eclipse, 1-3.9 hours partial eclipse, up to 3 times per year) are included in these results.

Since the radar DEM has error in terms of height and spatial placement, it is necessary to make an assumption of the proper error level to apply. Spatial error is not as critical, therefore no error is assumed. Regarding height error, for purposes of power system design, it is best to assume a conservative value. Reference 13 states the height error to be ±50 m. To be applied conservatively, the worse case height errors must be applied for both the shadowing terrain (increased by 50 m) and shadowed site (decreased by 50 m).

Figure 4 shows the worse case lunar day Site A1 data for both zero or the worse case height error. Although the patterns seem fairly similar, there are variations. One major difference (14 to 22° solar sublongitude) is due to a shadowing generating areal element which is very close to the height and location of Site A1. Adding worse case height error has the potential of shifting the shadowing terrain towards a more local cause rather than a distant one. This local shadowing terrain, in turn, affects the duration of the event, thus critically affects the minimum energy storage hours. In reality, it is unlikely the entire local areal element causes shadowing, since DEM height is an average over an entire area (i.e., there may be highly variable terrain slopes, boulders, rocks, or materials within one 600 by 600 m DEM pixel). A higher resolution DEM could address this problem.

Table 1 lists the average illumination fractions for various lunar days and energy storage hours for various recharge ratios. The table shows that values for the conservative (worse case) height error assumption are slightly worse than the “no error” case. Based on the desire to provide data for conservative power system design, all remaining analyses in this paper used the conservative error assumption.

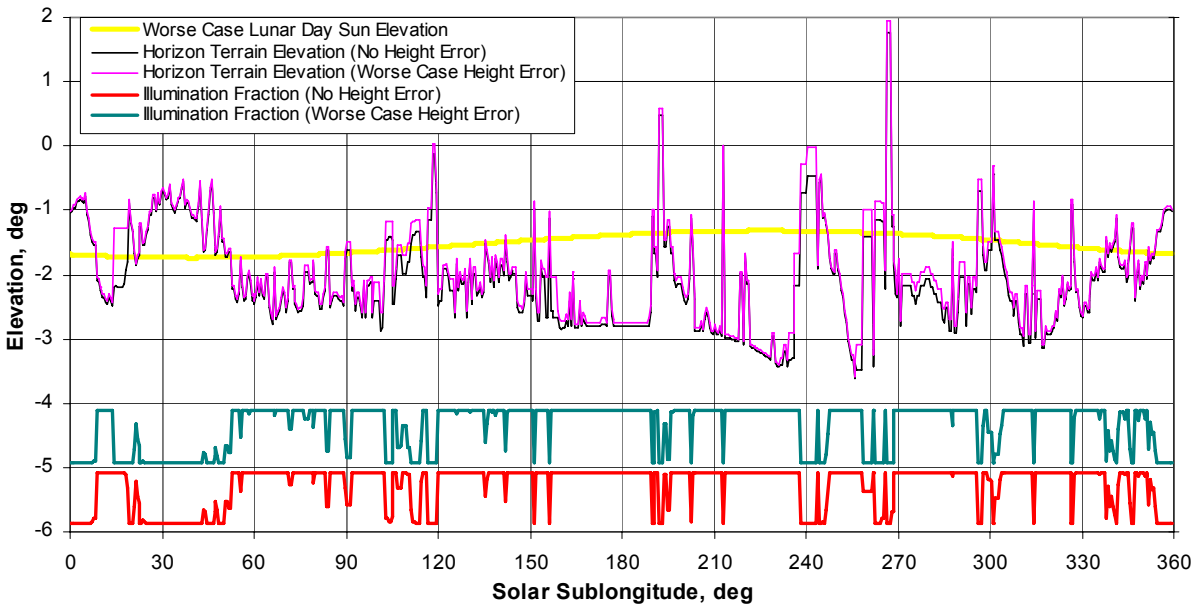

Figure 4.—Site A1 DEM height error comparison.

TABLE 1.—TABULATED DATA OF ANALYZED CASES

		Average Illumination Fraction				Worse Case Lunar Day Energy Storage Hours				
		Lunar Day				Recharge Ratio				
Site	Notes	Worse Case	1	2	3	4	2	1	0.5	0.25
A1	No Height Error	0.76	0.80	0.92	0.99	92	85	72	62	62
A1	With Height Error	0.71	0.75	0.90	0.98	117	103	94	81	73
A1	+ 100 m tower	0.76	0.80	0.92	0.99	92	85	72	62	62
A1	+ 200 m tower	0.79	0.82	0.94	0.99	88	80	70	60	60
A1	+ 400 m tower	0.83	0.86	0.96	0.99	78	73	63	56	56
A1	+ 800 m tower	0.87	0.90	0.98	1.00	66	59	48	43	43
A1	+ 1600 m tower	0.92	0.96	1.00	1.00	39	31	29	30	29
A2	With Height Error	0.57	0.62	0.77	0.89	231	169	86	66	66
A2	+ 400 m tower	0.75	0.80	0.93	0.99	86	77	66	59	59
A3	With Height Error	0.55	0.60	0.77	0.91	244	182	86	74	68
A3	+ 400 m tower	0.75	0.78	0.92	0.99	86	79	68	60	60
B	With Height Error	0.63	0.67	0.87	0.97	211	188	172	151	126
B	+ 400 m tower	0.78	0.82	0.95	0.99	110	91	75	58	58
C	With Height Error	0.60	0.67	0.81	0.93	261	257	249	233	212
C	+ 400 m tower	0.67	0.73	0.88	0.99	214	204	186	164	132
D	With Height Error	0.77	0.80	0.91	0.99	152	149	148	147	147
D	+Site reduced 1500 m	0.59	0.60	0.71	0.82	269	266	262	258	259
E	With Height Error	0.54	0.55	0.65	0.86	303	285	273	268	264
E	+ 400 m tower	0.61	0.63	0.75	0.90	268	264	262	260	256
F	With Height Error	0.70	0.72	0.83	0.96	162	157	145	121	100
F	+ 400 m tower	0.77	0.78	0.90	0.99	122	110	84	49	49
G	With Height Error	0.85	0.89	0.99	1.00	79	72	65	54	54
G	+Site reduced 1500 m	0.53	0.57	0.75	0.88	310	302	297	295	295
H	With Height Error	0.49	0.52	0.63	0.82	291	217	167	146	118
H	+ 400 m tower	0.66	0.68	0.80	0.94	134	121	94	56	56
A1+B	With Height Error	0.84	0.87	0.98	1.00	78	70	58	58	58
A1+B	+ 400 m towers	0.89	0.92	1.00	1.00	62	56	49	49	49
A1+C	With Height Error	0.86	0.91	0.99	1.00	64	55	51	42	36
A1+E	With Height Error	0.93	0.95	0.99	1.00	22	20	16	13	12
A1+F	With Height Error	0.91	0.93	0.99	1.00	42	39	39	39	39
A1+H	With Height Error	0.84	0.87	0.96	0.99	65	55	54	54	54

Other types of error have not been generally corrected in these analyses since they have not been adequately quantified. These include the error due to the averaging process for mountainous terrain (±50 m is only for flat terrain), general large scale correction offsets (based on lidar correlation and comparison with imagery), and erroneous specific areal elements (topographical outliers that do not seem to match imagery). The latter error have been addressed in specific site cases where the site itself seemed to have erroneous height.

Analysis Results: Site A1

Figure 5 shows the sun/horizon elevation and illumination fraction profile for Site A1 for the worse case lunar day, Lunar Day 1, Lunar Day 2, and Lunar Day 3 (to convert from solar sublongitude to site azimuth, subtract 213°). This figure enables one to compare and understand how illumination varies from one lunar day to the next and understand which times of the lunar day has shadowing and when it diminishes. At 120°, the peak is caused by Site F terrain about 32 km away. At 192°, the peak is caused by Site D terrain about 54 km away. At 266°, the peak is caused by Site G terrain about 29 km away. The critical shadowing from -6 to +50° is discussed later in this section.

Figure 6 shows the average illumination and energy storage duration for various power system types throughout the year for Site A1. The start time is referenced from 2/2/94 (the start of the worse case lunar day). The illumination fraction and energy storage hours for the given time is the average over the subsequent 711 Earth hours. For a large portion of the year, there is a small amount of shadowing (determined to be caused by Site G which is shown later in the paper to likely be erroneously high).

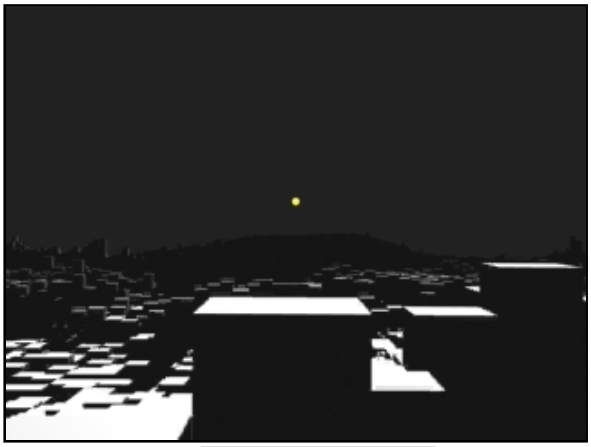

Play movie

(An animation of a viewer's or solar array's perspective located at Site A1 for an entire lunar day is shown above (the video animation can be viewed within the .pdf file online at http://gltrs.grc.nasa.gov). The viewpoint is 50 m above Site A1's surface and tracks the Sun's azimuth. This animation shows the actual, unsmoothed, radar digital elevation model rendered using a 3–D modeller with ray-traced shadow casting for 1 hour time steps. The 600 by 600 m DEM pixels appear as blocks; it is not technically valid to smooth these average height data pixels even though aesthetically it would be more appealing. Importantly, this illustrates that higher resolution pixels are needed for nearby terrain and site terrain while being less important for distant terrain. The animation begins with the view of Malapert Mountain. The lower dot near the horizon is the worse case lunar day Sun position and the higher dot is the best case lunar day Sun position. The best case was used for rendering the illumination/shadowing animation. During the last half of the animation, the adjacent dark Shackleton Crater is shown with its illuminated rim bounding the region. Near the end of the animation it is apparent that the worse case lunar day Sun is blocked for extended durations by distant terrain.)

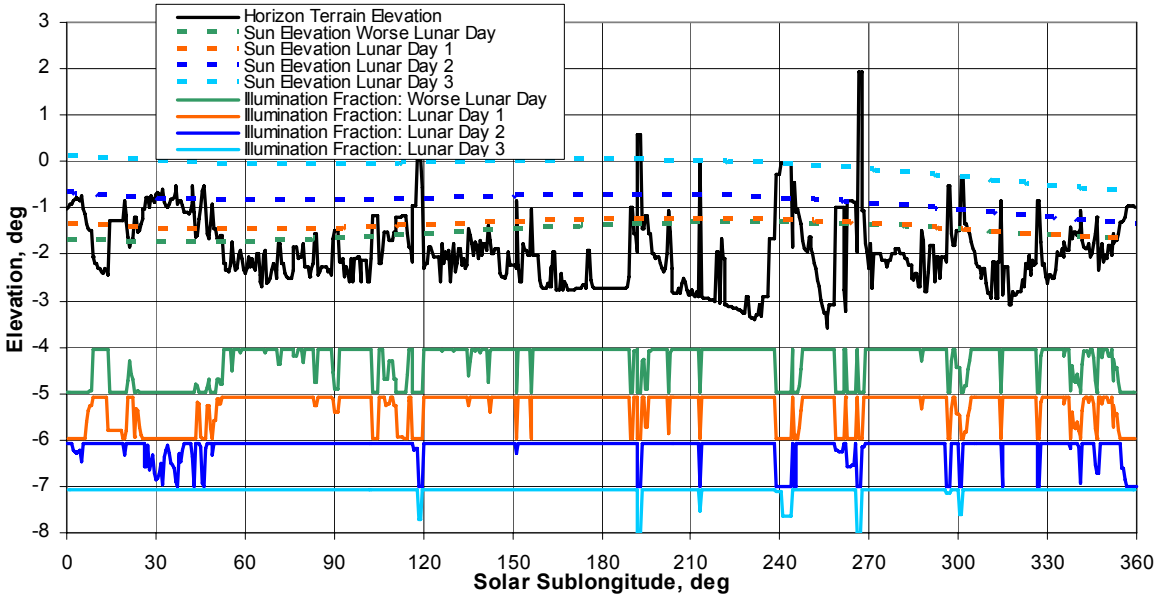

Figure 5.—Site A1 elevation and illumination fraction profiles.

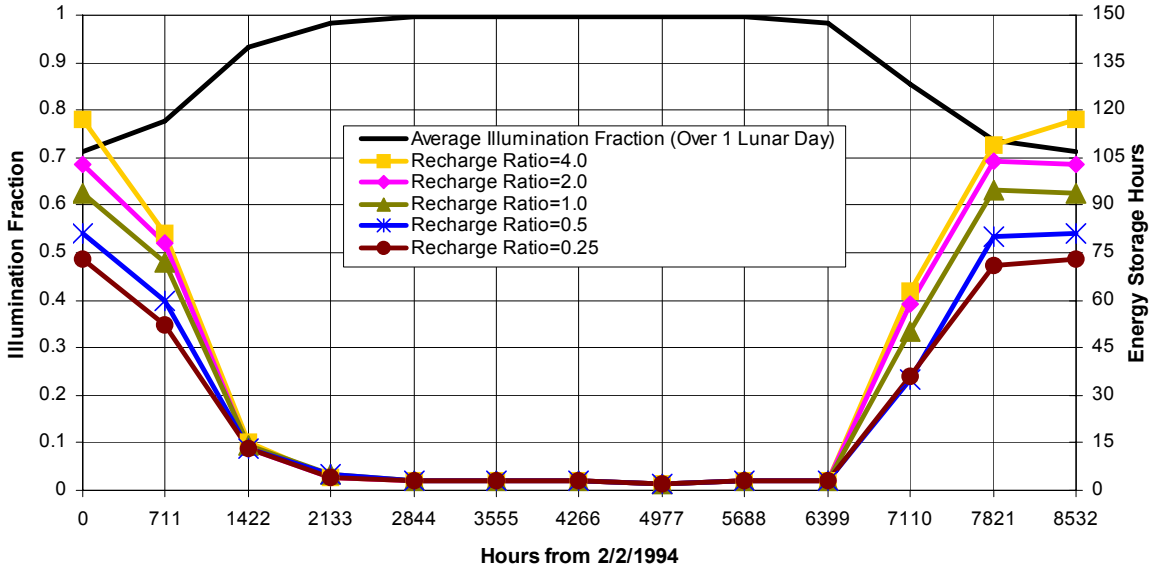

Figure 6.—Annual effect of Sun elevation on Site A1 illumination fraction and energy storage hours.

To understand what terrain is shadowing onto Site A1, figure 7 shows a white line on a background radar backscatter image (ref. 14) which spatially depicts the highest terrain (i.e., the horizon terrain elevation) as viewed from the site. The terrain that is shadowing Site A1 on the worse case lunar day is shown as blue dots. Also shown on the figure are the terrain heights (relative to 1737.4 km lunar reference radius). Near solar sublongitudes of -10 to 50° are distant high terrain (Malapert Mountain is from -10 to 7°) that contribute sizable shadowing at shallow solar elevation angles. From 250 to 290° are a variety of relatively close shadow casting terrain.

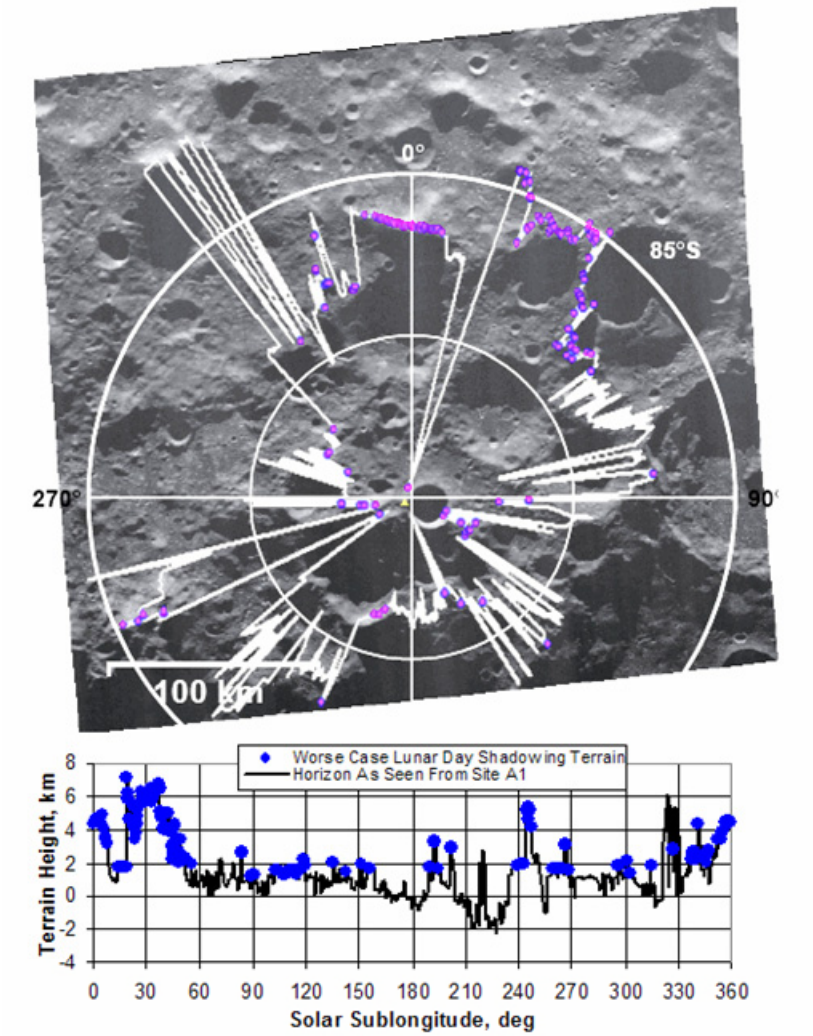

Figure 7.—Site A1 terrain horizon height and shadowing terrain for worse case Lunar Day.

According to the Site A1 analysis for Lunar Day 1, the critical energy storage period occurs during a solar sublongitude range from -6 to 50° (note that illumination fractions lower than 0.50 are considered fully shadowed for this purpose). It is important to confirm that the distant terrain is actually inducing this shadowing during this period because for the worse case lunar day, the shadowed period is even longer. Figure 8 illustrates this critical period with key images from Clementine. For Lunar Day 1, the only available Clementine images that can be used to verify the shadowing from the Malapert Mountain region are images from orbit 150 (solar sublongitude = 48°) to orbit 162 (solar sublongitude = 18°). Images from orbits 154 to 158 (solar sublongitude = 38 to 28°), 161 (21°), 163 (16°), 166 (7°), and 168 (2°) are either black or have no illumination on Crater Shackleton. Images from orbits 150, 152 (solar sublongitude = 43°) and 160 (solar sublongitude = 23°) are highly shadowed at Crater Shackleton. The image for orbit 162 is fairly well lit over a reasonably sized area. To explain the orbit 162 illumination, examination of figure 7 shows a “gap” in the distant terrain (between Malapert Mountain and the other high terrain) near solar sublongitude of 18° which allows illumination over a larger area of the Crater Shackleton area. An image from orbit 148 (solar sublongitude = 53°) is also shown. Not shown on figure 8 is an image from orbit 169 (solar sublongitude = 0°) which includes the shadowing of Crater Shackleton from Malapert Mountain.

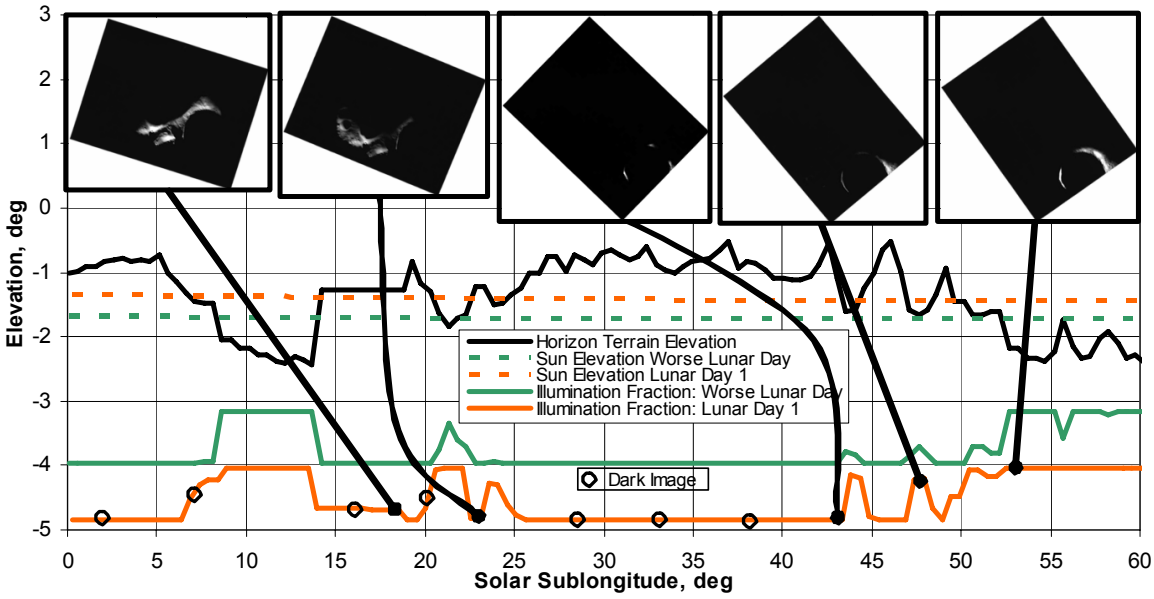

Figure 8.—Matching of critical terrain shadowing with Site A1 analysis results.

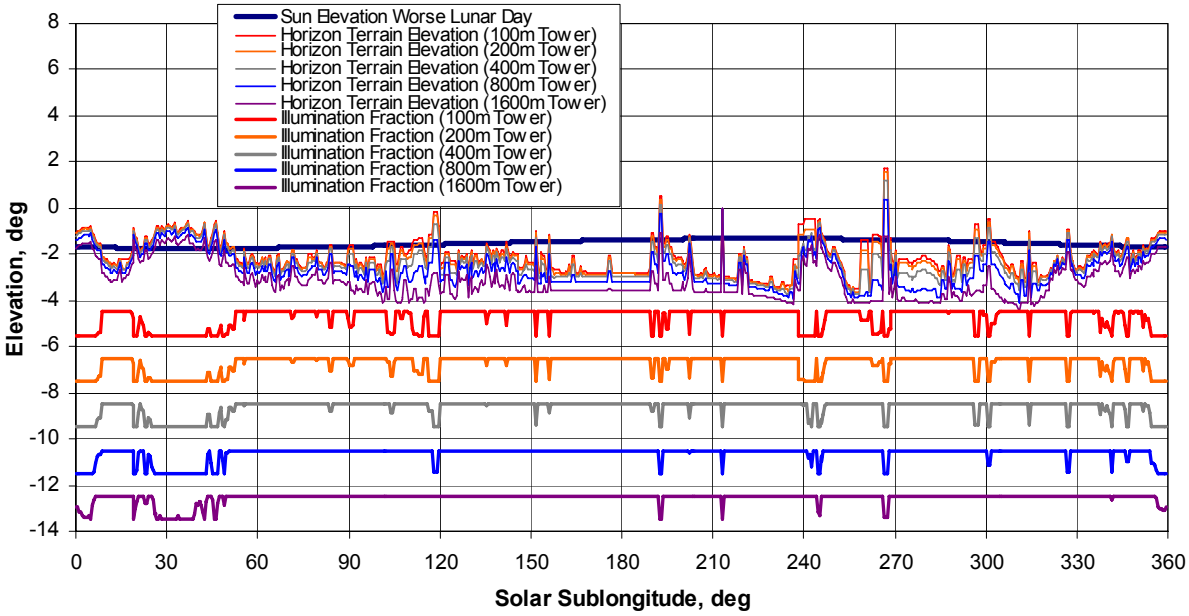

Figure 9.—Elevations and illumination fraction profiles for Site A1 with various tower heights.

Analysis Results: Usage of Towers

Figure 9 shows the illuminated energy profiles and horizon terrain elevations as seen from the top of various tower heights at Site A1 for the worse case lunar day. This kind of analysis is not practical using the imagery analysis method; it is only possible using a DEM.

Figure 10 shows a plot of average illuminated energy and energy storage durations as function of tower height for the worse case lunar day at Site A1.

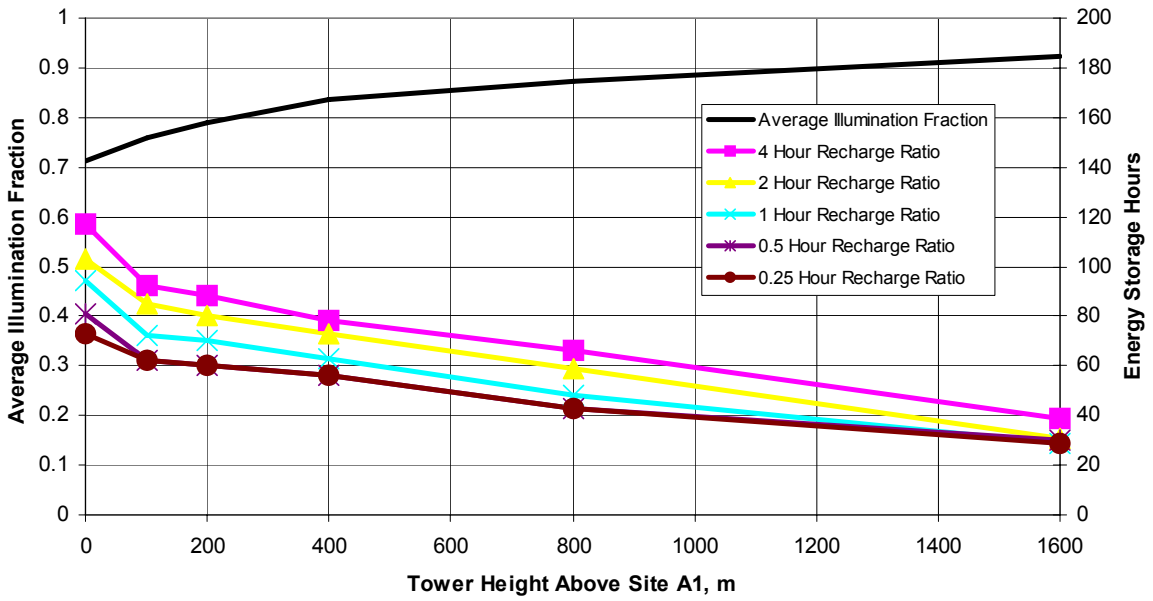

Figure 10.—Effect of tower height on illumination fraction and energy storage hours.

Up to a 1600 m high tower (an assumed height limit based on extrapolating terrestrial tower designs, which are as high as 650 m, to a low gravity lunar application), the energy storage time is reduced to 29 hours (a 3.1 km tower is needed to eliminate the energy storage caused by terrain shadows). The primary shadowing terrain is still the region near Malapert Mountain which is so high that shallow sun angles result in shadows that are hard to avoid. A more reasonably sized tower (100 m) can reduce the energy storage time from 11 to 25 hours (or 15 to 21 percent reduction from ground level). The greatest improvement in energy storage time comes from tower increases up to 100 m. Depending on recharge ratio, the reduction of recharge storage hours required can go from 0.12 to 0.25 'energy storage hours reduction'/meter. However, above the 100 m, this improvement rate reduces to 0.022 to 0.036 'energy storage hours reduction'/meter. This is mainly due to the lower height (briefer shadowing inducing) terrain being alleviated by the higher tower height. A detailed mass analysis is required to determine whether utilizing a tower is a mass optimum solution (terrestrial towers are quite heavy at about 600 kg/m for ~600 m steel, guy-wire-supported TV communications towers).

Analysis Results: Other Sites

In the subsequent figures, the illumination profile is shown for the worse case lunar day. Along with the horizon terrain elevation profile, the worse case lunar day, Lunar Day 1, Lunar Day 2, and Lunar Day 3 sun elevation is shown. These are provided as a function of solar sublongitude. The illumination fraction profile is read such that a high value is illuminated, a low value is shadowed and a linear variation in between indicating partial solar blockage. A summary of the average illumination fractions and the worse-case lunar day energy storage hours for these cases is provided in table 1.

Figure 11 illustrates the analysis data for Site A2 (to convert from solar sublongitude to site azimuth, subtract 237°). (Site A3 has similar profiles to Site A2 therefore it's profiles are not duplicated.) The elevation peak from 177 to 187° is due Site A1 (~3 km away). The elevation peak from 26 to 37° is due other Crater Shackleton rim terrain (~4 km away). The peak at 260° is due to Site G about 30 km away. As was seen with Site A1 results, because local terrain is causing some shadowing, the resolution limitation of the DEM is apparent (i.e., since a local DEM pixel is one average height, it appears like a flat plateau). One adjacent DEM pixel can block relatively large swath of solar sublongitude due to its

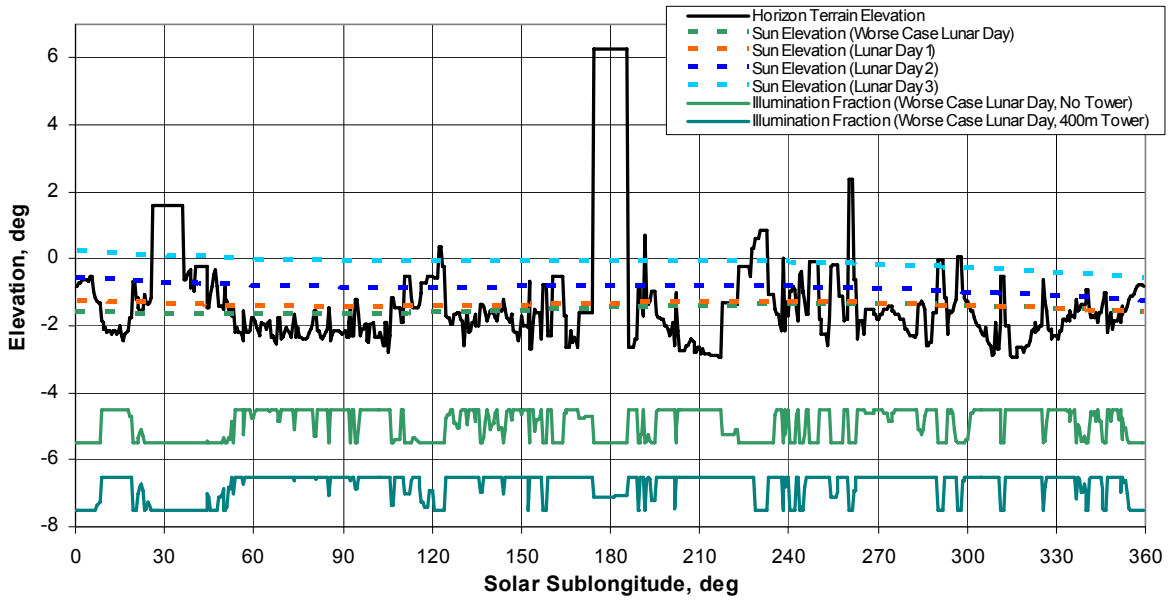

Figure 11.—Site A2 elevation and illumination fraction profiles.

fixed average height. In reality, at a higher resolution, this pixel-area may have almost any shape including highly jagged terrain, gently sloping hills, and a few high peaks with large lower areas. The assumption of worse-case, conservative error (which makes nearby DEM pixels higher than the site) enhances the likelihood of local terrain casting shadow on a site. The farther the terrain is from the site, the less of a problem the pixel resolution/height averaging is. For example, at 143 km, an areal element (pixel) can block up to 1.0° of solar sublongitude (effectively, 2 Earth hours), at 16.5 km this increases to 2.0° (4 hours) and at 1.4 km it is 25° (49 hours). Without better resolution DEMs to eliminate these local "plateaus," the analysis of blockage due to nearby terrain may effectively be overestimating the shadowing, although this is acceptable because the results are conservative. Adding a 400 m high tower reduces the energy storage time to 59 hours (a 3.2 km tower is needed to eliminate the energy storage required during terrain shadows).

Figure 12 illustrates the analysis data for Site B (to convert from solar sublongitude to site azimuth, subtract 233°). There is an adjacent high terrain area element which, if adjusted based on the worse case error assumption, would have a height sufficient for shadowing/blockage for a relatively long swath of solar sublongitudes (the main limitation from applying such offsets to adjacent DEM terrain). Thus, for this one site, the adjacent elemental area terrain was assumed to be adjusted in the same direction as the site. For 150 to 240°, the slightly curved baseline is due to absent radar DEM terrain height data. When generating elevation profiles, the region outside the radar DEM is assumed to be the reference lunar height, therefore for cases with sites near this region or where there is much low height terrain between the site and the outside region, then it is likely that the reference height will be the cause for blocking the sun. The peak from 60 to 70° is due to Site A1 and other high terrain (1.5-2 km height) from 2 to 13 km away. The peak at 180° is due to the high terrain of Site D about 47 km away. The peak at 280° is due to the high terrain of Site G about 20 km away. Adding a 400 m high tower reduces the energy storage time from 126 to 58 hours for a fast recharge power system (a 3.5 km tower is needed to eliminate the energy storage required during terrain shadows).

Figure 13 illustrates the analysis data for Site C (to convert from solar sublongitude to site azimuth, subtract 293°). The peak near 160° is due to Site G about 25 km away. Adding a 400 m high tower reduces the energy storage time from 212 to 132 hours for a fast recharge power system (a 3.7 km tower is needed to eliminate the energy storage required during terrain shadows).

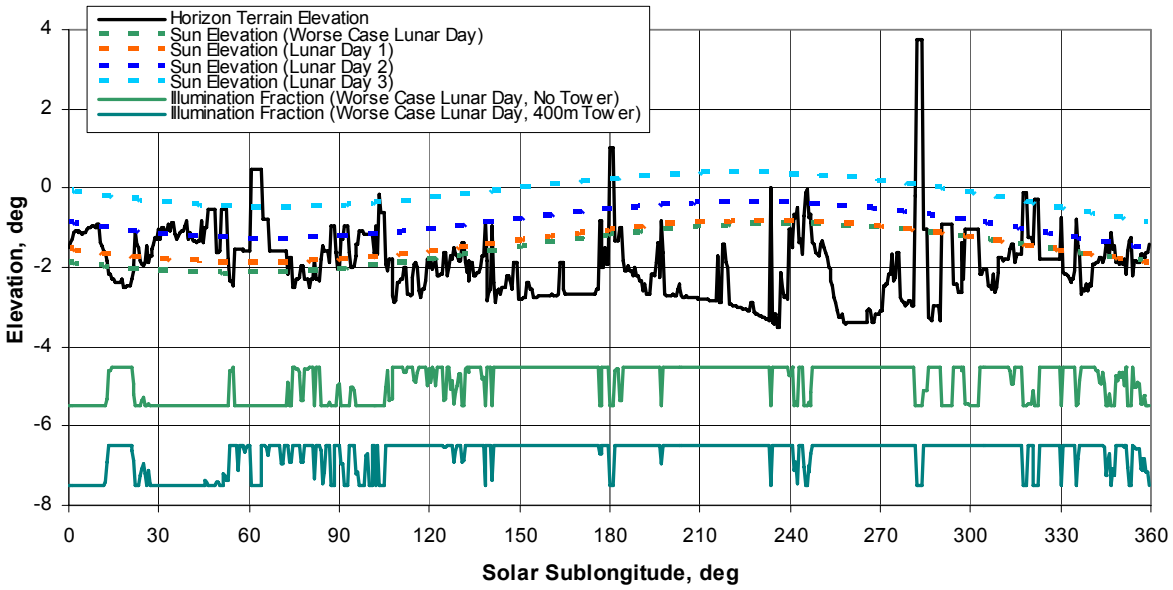

Figure 12.—Site B elevation and illumination fraction profiles.

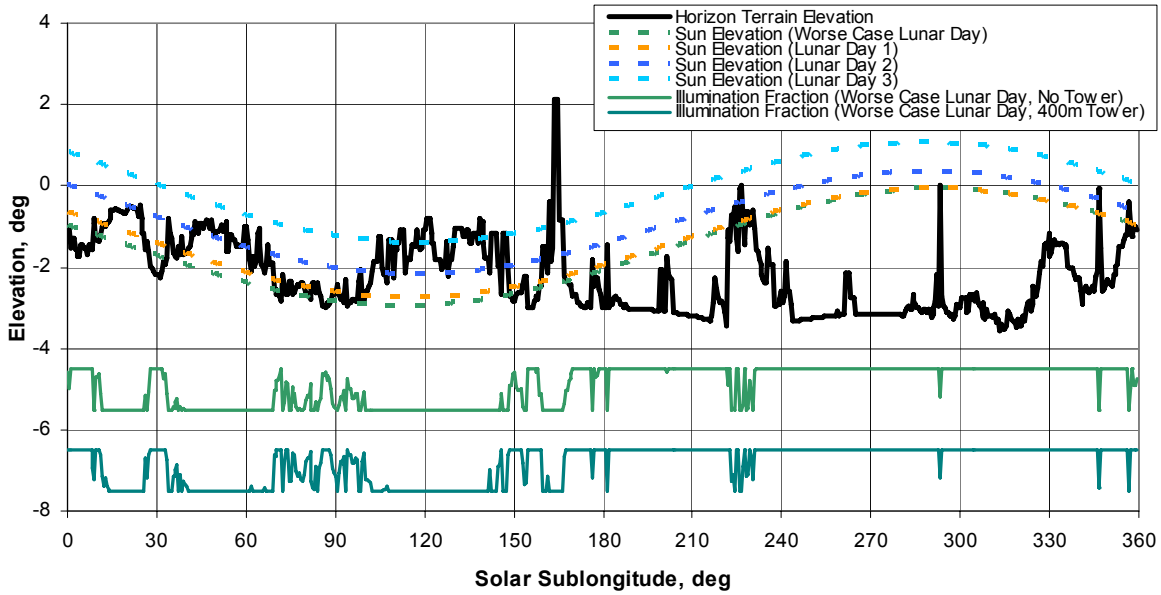

Figure 13.—Site C elevation and illumination fraction profiles.

Figure 14 illustrates the analysis data for Site D (to convert from solar sublongitude to site azimuth, subtract 195°). From 120 to 250°, the slightly curved baseline is due to a combination of site height and absent radar DEM terrain heights (whose heights must then be assumed to be the standard lunar reference height). This site appears to be the peak of a slope (3.2 km height) with the highest adjacent area element (as shown in the radar DEM, other radar-blocked data may be higher) being 1.4 km high. Although this site may be ruled out simply because this peak is potentially impossible to traverse due to steep slopes, the more likely possibility is that it is an erroneous radar DEM height pixel. Although this seems unlikely since the data are averaged over 16 higher resolution area subelements, Lunar Day 1 and 2 images were examined and compared with the illumination profiles. No obvious illuminated pixel corresponded to the

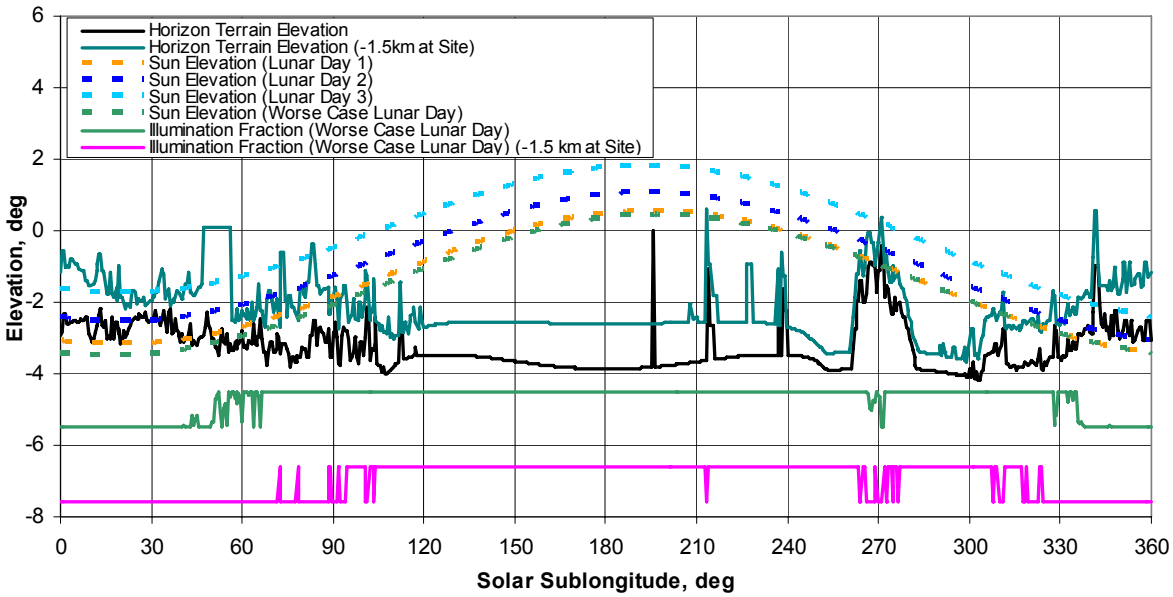

Figure 14.—Site D elevation and illumination fraction profiles.

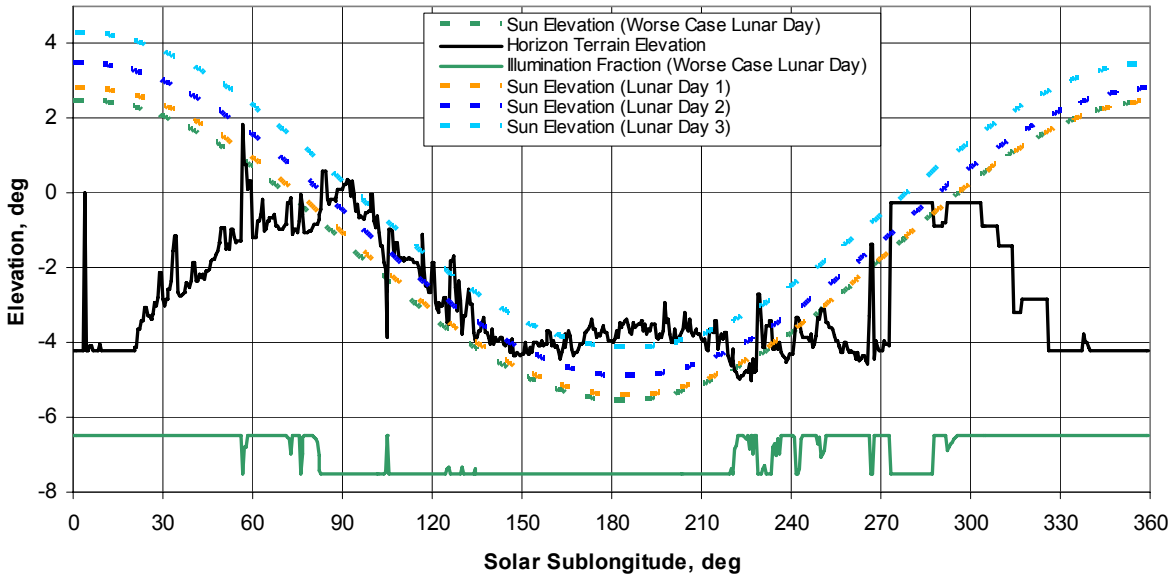

Figure 15.—Site E elevation and illumination fraction profiles.

one radar DEM pixel of Site D. It is possible that the resolution of the imagery was insufficient to show high radar DEM pixel. Iterating the radar DEM Site D height and using the computer program to try to match the imagery-derived illumination profile of the site showed that the height of the site is likely 1.5 km too high. As seen in table 1, assuming a 1.5 km site height reduction, reduces the average illumination fractions significantly and increases the energy storage hours, a more likely result based on imagery examination.

Figure 15 illustrates the analysis data for Site E (to convert from solar sublongitude to site azimuth, subtract 5°). There is much high mountainous terrain near this site. From 50 to 140°, the shadowing terrain is due to terrain from 50 to 100 km away from 2.3 to 7.1 km high. From 274 to 300°, the shadowing terrain is very close (from 2 to 6 km away) and 4.1 to 4.7 km high. From 160 to 210°, the shadowing terrain is near Crater Shackleton. The data was reassessed monthly from 1994 to 2030 and the

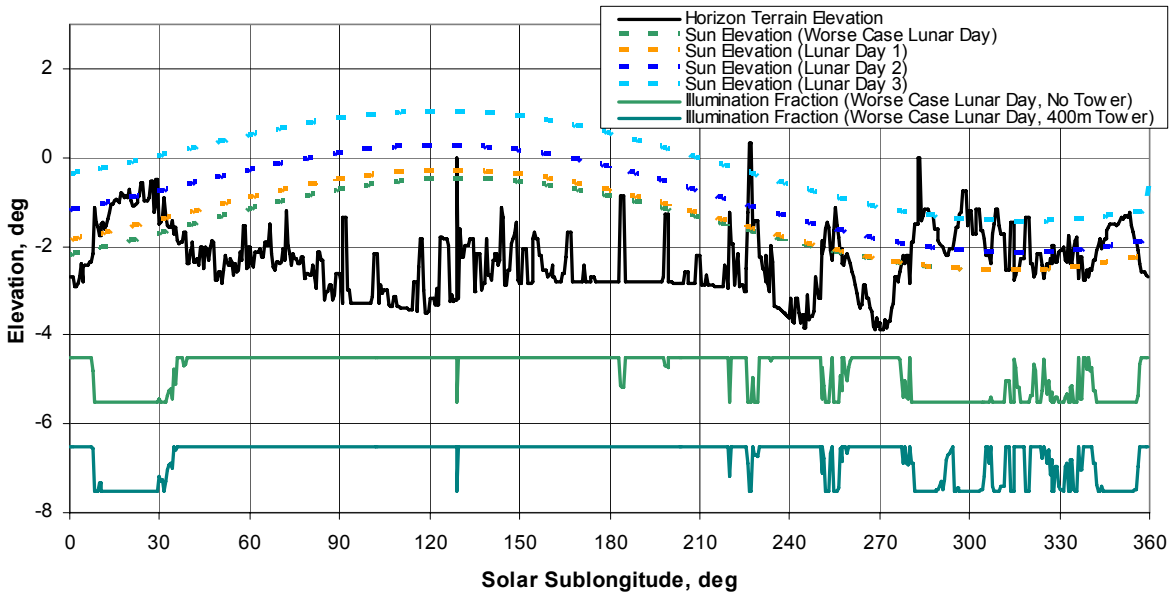

Figure 16.—Site F elevation and illumination fraction profiles.

peaks were cyclically similar, thus the worse case shown is typical. Adding a 400 m high tower reduces the energy storage time from 264 to 256 hours for a fast recharge power system (a 5.9 km tower is needed to eliminate the energy storage required during terrain shadows). Although a tower can potentially eliminate terrain shadowing in other assessed sites, due to the fact that the Sun elevation goes so low for the worse case lunar day (-5.5°) and the relatively high terrain near Shackleton Crater, then a much higher tower is needed to eliminate terrain shadowing from that area.

Figure 16 illustrates the analysis data for Site F (to convert from solar sublongitude to site azimuth, subtract 130°). For 280 to 360°, the shadowing terrain is due mainly to terrain near/including Sites A1, B, C, and G. The high point at 228° is Site D. For 10 to 40°, the shadowing terrain is caused by Site E and terrain near it. Adding a 400 m high tower reduces the energy storage time from 100 to 49 hours for a fast recharge power system (a 3.1 km tower is needed to eliminate the energy storage required during terrain shadows).

Table 1 shows that Site G had very high average illumination fractions and very low energy storage hours. Site G was identified as a potential site based on its radar DEM height (3.0 km) compared to other terrain heights within 20 km of it (especially, the highest adjacent elemental area of 1.9 km height). Like Site D, although this site may be ruled out simply because it may be an inaccessible small mountain peak, it seems likely that it is an erroneous radar DEM height pixel. Lunar Day 1 and 2 images were examined and compared with the illumination profiles. Unique high pixels that correspond to the radar DEM pixel for Site G do not appear. As with Site D, it is possible that the resolution of the imagery is not sufficient to show a small area “peak”. Iterating the radar DEM Site G height and using the computer program to try to match the imagery-derived illumination profile of the site showed that the height of the site is likely 1.5 to 2 km too high. As shown in table 1, assuming 1.5 km site height reduction reduces the average illumination fractions and increases the energy storage hours significantly.

Figure 17 illustrates the analysis data for Site H, which is near the opposite side of the Shackleton Crater from Sites A1 to A3 (to convert from solar sublongitude to site azimuth, subtract 121°). For 260 to 324°, the shadowing terrain is due mainly to terrain near/including Sites A1, B, C, and G. From 200 to 220°, the shadowing is due to adjacent terrain. Site F causes the shadowing at 140°. For 12 to 43° and 340 to 360°, the shadowing terrain is caused by Site E and terrain near it. Adding a 400 m high tower reduces the energy storage time from 118 to 56 hours for a fast recharge power system (a 3.4 km tower is needed to eliminate the energy storage required during terrain shadows).

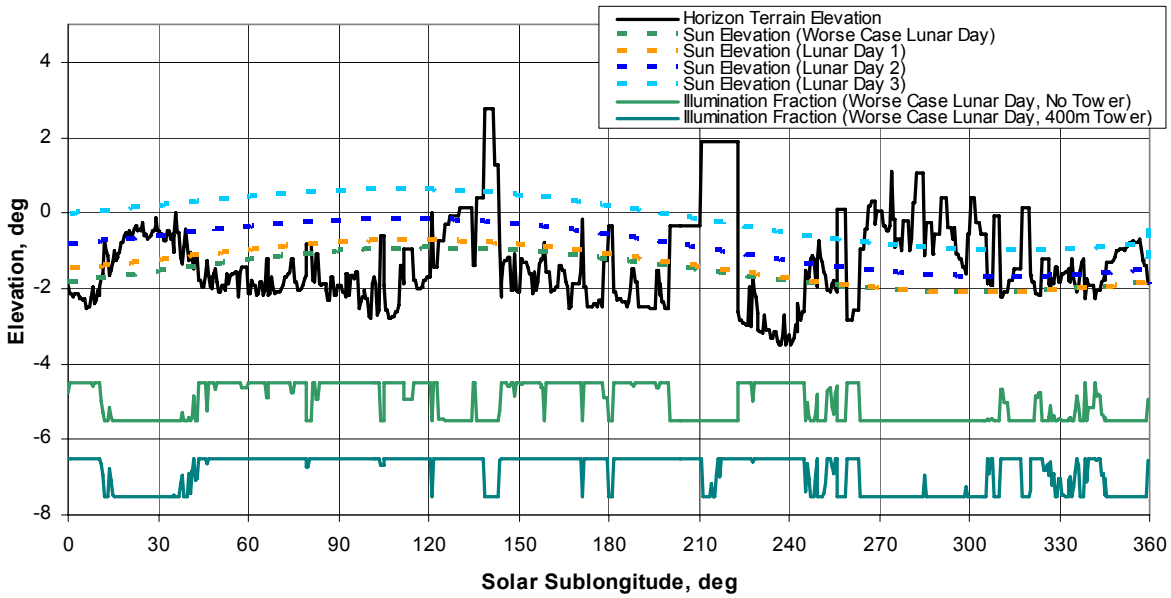

Figure 17.—Site H elevation and illumination fraction profiles.

Analysis Results: Site Interconnection

References 2 to 9 suggest (based on Lunar Day 2 analysis) that combining the illumination of Sites A1 and B (via power cables or beaming over the ~10 km distance) could provide energy generation up to 98 percent of the time. The operational and engineering complexities of deployment/development of such a concept will not be discussed here. However, it is necessary to evaluate the concept for the worse case lunar day (rather than two lunar days past this time) and from the viewpoint of energy storage duration. Figure 18 shows the individual Site A1 and B illumination profiles as well as their combination. Note that when combining the sites, it is assumed that energy greater than 1.0 is not used. The worse case lunar day average illumination fraction for Site A1 is 0.71, Site B is 0.63 and the combined value is 0.84. The worse-case lunar day energy storage hours are 68, 62, 58, 58, and 58 for recharge ratios of 4, 2, 1, 0.5, and 0.25, respectively. This compares favorably with the independent values for Site A1 and B.

Connecting two sites improves the average illumination and energy storage hours. Both Sites A1 and B are shadowed by similar worse case shadowing terrain except they are time shifted (for 20 to 50°, the distant, high shadowing terrain covers both sites). In order to be very competitive in a mass optimized power system trade space, it is likely that a nearly continuous combined illumination condition is required (thus nearly eliminating energy storage). However, to accomplish this would likely require an operationally prohibitive site separation even greater than 10 km and/or utilization of mass-intensive towers. Figure 18 also shows the effect of connecting Sites A1 and B as well as using 400 m towers at both sites. Even with adding 400 m towers, some shadowing due to the standard high mountainous terrain near Malapert Mountain is unavoidable. Figure 19 shows the illumination fraction for connecting Sites A1/C, A1/E, A1/F and A1/H. The widest separated sites (A1 and E) have the best combined illumination, although they may be impractical to connect.

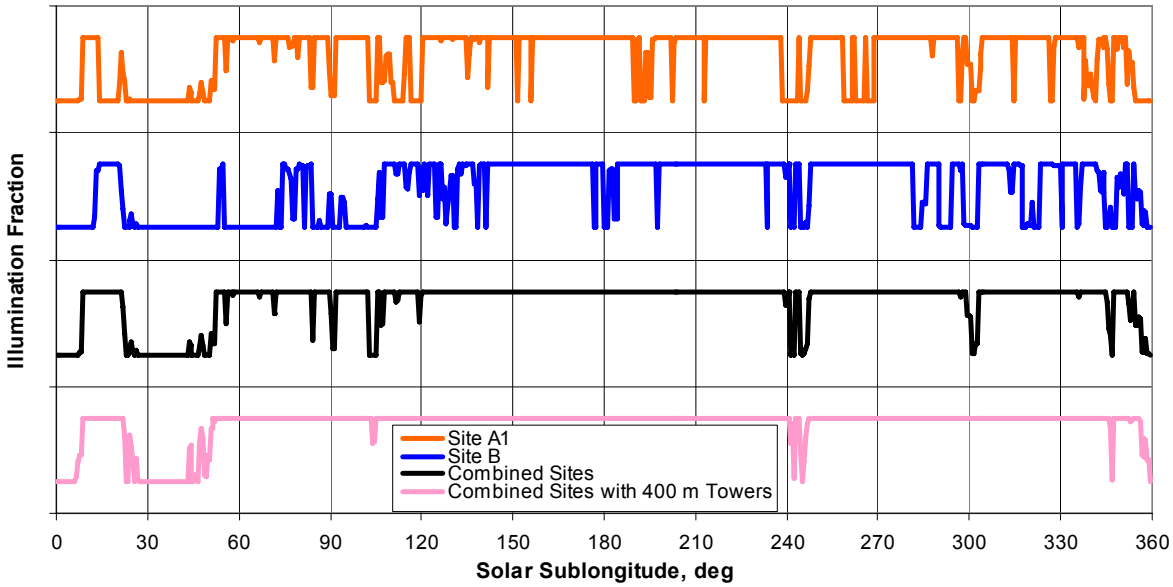

Figure 18.—Combined illumination of Sites A1 and B.

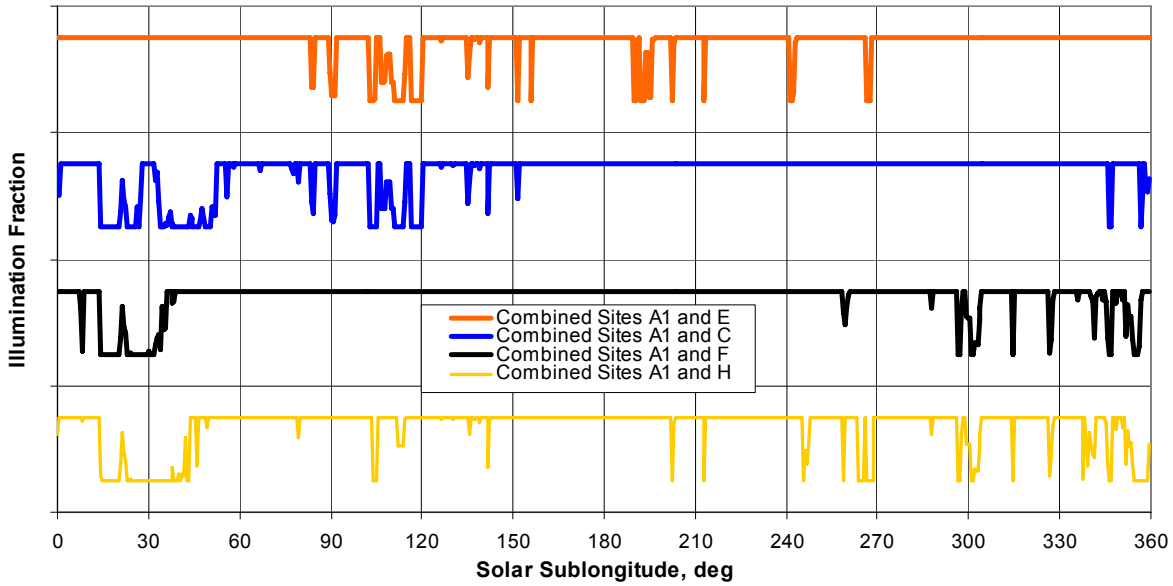

Figure 19.—Illumination profile for other combined sites.

Future Work

Several possible avenues may be pursued to enhance the quality of future illumination analyses. Primarily, higher resolution radar DEMs would be of great help (currently being developed at JPL and should be available in 2007). Obtaining access to SMART-1 imagery of the lunar polar regions for the entire year, especially for the worse case lunar day, would be very useful (these data are still being processed without a clear completion date). Of course, anticipated future surface radar and image mapping lunar missions whose results may become available in upcoming years will provide added temporal and spatial coverage and resolution.

Merging the radar DEM with the Smithsonian DEM to address the missing height data areas may enhance the results, especially near the radar DEM edges where some other candidate high illumination sites were found. Additionally, a more detailed assessment of the radar DEM could be performed to remove or correct specific high shadow causing area elements (e.g., Sites D and G) as well as make more general corrections which would enhance comparisons with available imagery. Enhancement of the partial Sun blockage algorithms to consider vertical blockage (instead of only horizontal blockage as currently implemented) would further enhance the illumination estimates.

In addition to the lunar south pole region, DEMs are available for future analysis of lunar north pole sites as well as sites not near the polar regions.

Other useful products of the illumination analysis tool that could be produced in the future would be a energy storage map for the worse case lunar day (and others) analogous the average illumination map produced by Bussey for Lunar Day 2 and a creation of the average illumination map for the worse case lunar day.

In addition to illumination analysis, the author has adapted and utilized the analysis method with the radar DEM to quantify Site A1 communication coverage blockage of terrestrial sites by lunar horizon terrain (results quantified the timing, duration, and cause of the blockage of Earth communications sites by lunar terrain, namely Malapert Mountain).

Conclusion

This paper has provided a review of past work in the lunar polar illumination area and documented an analysis of potential high illumination sites, which may be considered for manned or unmanned operations, using an independently developed computer program and a radar DEM. This paper has clarified and extended the findings of the other researchers in the field whose results might have been misinterpreted. The radar DEM has been determined to provide adequate accuracy for preliminary illumination quantifications, although it has the potential for improvement by way of various height corrections. The results shown in this paper have been formulated to be used by power system designers to perform mass optimized sizing of solar and energy storage systems. The sun/shade times depicted provide useful engineering data enabling detailed analysis and design of various lunar polar based systems. This paper confirms the results of previous researchers that Site A1 has the most favorable illumination characteristics of the region. A significant contribution, inherent in using DEM analysis methods, was the definition, location, and quantification of the shadow-inducing terrain for the worse-case energy storage hours periods, an aspect that was seemingly omitted in imagery analyses due to apparent lack of Clementine imagery for the periods (i.e., dark or black images were shadowed instead being ‘faulty’). Interesting counter-intuitively lower illumination results for the Malapert Mountain peak site were presented. Significantly, two sites, although seemingly of higher illumination than Site A1, appear to have erroneous radar DEM heights, the elimination of which would, significantly, permit continuous illumination of Site A1 during some months of the year. Two key contributions of this paper include the assessment of the illumination benefit 1) of site height increases using a tower at various sites and 2) of combining the illumination of the various sites (as well as adding towers to these combined sites). Of concern is the uncertainty of illumination analysis results due to low resolution radar DEM data (emphasized by Site A2 local shadowing terrain which appears flat since it is the average height, but which may be much different) and the revealed potential error in the radar DEM (as seen in Sites D and G altitudes being likely too high). These erroneous points (and other such pixels) may be corrected to reduce any shadowing they cause on other sites although it is not clear what other general height corrections can be applied to the radar DEM and whether they increase or decrease the illumination for each site although initial comparisons with imagery suggest lowering the heights at and around Site A1would reduce the average illumination.

References

1. Spudis, P.D., Stockstill, K.R., Ockels, W.J., and Kruijff, M., "Physical Environment of the Lunar South Pole from Clementine Data: Implications for Future Exploration of the Moon," Abstracts of the Lunar and Planetary Science Conference, Vol. 26, 1995, pp. 1339–1340.
2. Bussey, D.B.J., Spudis, P.D., and Robinson, M.S., "Illumination Conditions at the Lunar South Pole," Geophysical Research Letters, Vol. 26, No. 9, May 1999, pp. 1187–1190.
3. Bussey, D.B.J., Robinson, M.S., Edwards, K., Cook, A.C., and Watters, T., "Simulation of Illumination Conditions at The Lunar South Pole," 32nd Annual Lunar and Planetary Science Conference, Mar. 2001, Abstract 1907.
4. Fristad, K., Bussey, D.B.J., Robinson, M.S., and Spudis, P.D., "Ideal Landing Sites near the Lunar Poles," 35th Lunar and Planetary Science Conference, Mar. 2004, Abstract 1582.
5. Bussey, D.B.J., Robinson, M.S., Fristad, K., and Spudis, P.D., "Permanent Sunlight at the Lunar North Pole," 35th Lunar and Planetary Science Conference, Mar. 2004, Abstract 1387.
6. Bussey, D.B.J., and Spudis, P.D., "The Lunar Polar Illumination Environment: What We Know & What We Don't," Proceedings of Space Resources Roundtable VI, Lunar and Planetary Institute, Nov. 2004, LPI Contribution 1224, pp. 14.
7. Bussey, D.B.J., Robinson, M.S., and Spudis, P.D., "Illumination Conditions at the Lunar Poles," 30th Annual Lunar and Planetary Science Conference, Mar. 1999, Abstract 1731.
8. Bussey, D.B.J., and Spudis, P.D., "Extreme Lighting Conditions At The Lunar Poles," AAS 03–717, Proceedings of the International Lunar Conference 2003, Exploration Working Group 5, Nov. 2003, pp. 125.
9. Bussey, D.B.J., Robinson, M.S., and Spudis, P.D., "Clementine High Resolution Imaging of the Lunar South Pole," 30th Annual Lunar and Planetary Science Conference, Mar. 1999, Abstract 1738.
10. Bussey, D.B.J., and Spudis, P.D., "The Lunar Poles: Mapping the Future Lunar Base," Proceedings for the International Conference Moon Base: a Challenge for Humanity, May 2005.
11. de Weerd, J.F., Kruijff, M., and Ockels, W.J., "Search for Eternally Sunlit Areas at the Lunar South Pole From Recent Data: New Indications Found," 49th International Astronomical Congress, IAF–98–Q.4.07, Sept 1998.
12. Kruijff, M., "Peaks of Eternal Light on the Lunar South Pole: How They Were Found and What They Look Like," 4th International Conference on Exploration and Utilization of the Moon, ESTEC, ESA SP–462, July 2000, pp. 333.
13. Margot, J.L., Campbell, D.B., and Slade, M.A., "Digital Elevation Models of the Moon From Earth-Based Radar Interferometry," IEEE Transactions on Geoscience and Remote Sensing, Vol. 38, No. 2, Mar. 2000, pp. 1122–1133.
14. Margot, J.L., Campbell, D.B., Jurgens, R.F., and Slade, M.A., "Topography of the Lunar Poles from Radar Interferometry: A Survey of Cold Trap Locations," Science, Vol. 284, Issue 5420, Jun. 1999, pp. 1658–1660.
15. Rosiek, M.R., Kirk, R., and Howington-Kraus, E., "Digital Elevation Models Derived From Small Format Lunar Images," ASPRS 2000 Annual Conference, May 2000.
16. Rosiek, M.R., Kirk, R., and Howington-Kraus E., "Lunar South Pole Topography Derived From Clementine Imagery," Workshop on New Views of the Moon II: Understanding the Moon Through the Integration of Diverse Datasets, Lunar and Planetary Institute, Sept. 1999, Abstract 8046, pp. 52.
17. Cook, A.C., Spudis, P.D., Robinson, M.S., Watters T.R., and Bussey, D.B.J., "The Topography of the Lunar Poles from Digital Stereo Analysis," 30th Annual Lunar and Planetary Science Conference, Mar. 15–29, 1999, Abstract 1154.
18. Cook, A.C., Oberst, J., Roatsch, T., Jaumann, R., and Acton, C., "Clementine Imagery: Selenographic Coverage for Cartographic and Scientific Use," Planetary and Space Science, Vol. 44, No. 10, 1996, pp. 1135–1148.

19. Spudis P.D., Cook, A.C., Robinson, M.S., Bussey, D.B.J., and Fessler, B., "Topography of the South Polar Region From Clementine Stereo Imaging," Workshop on New Views of the Moon, Lunar and Planetary Institute, 1998, pp.79–80.
20. Garrick-Bethell, I., Byrne, S., Hoffman, J.A., and Zuber, M.T., "Areas of Favorable Illumination at the Lunar Poles Calculated from Topography," 36th Annual Lunar and Planetary Science Conference, Mar. 14–18, 2005, Abstract 2006.
21. Kruijff, M., "Visibilities and Lighting Conditions on a Modeled Lunar Surface," EWP 1819, ESA/ESTEC/WGS, Noordwijk, Netherlands, 1995.
22. Shillcutt, K., "Solar Based Navigational Planning for Robotic Explorers," Ph.D. Thesis, Robotics Institute, Carnegie Mellon University, Oct. 2000, CMU–RI–TR–00–25.
23. Shillcutt, K., and Whittaker, W., "Solar Navigational Planning for Robotic Explorers," Proceedings of the 2001 IEEE International Conference on Robotics and Automation, May 2001, pp. 1421–1426.
24. Shillcutt, K., and Whittaker W., "Solar Power Expert for Remote Robotic Explorers," Proceedings of the International Symposium on Artificial Intelligence, Robotics and Automation in Space, Jun. 1999, ESA SP–440, pp. 243.
25. Sharpe, B.L., and Schrunk, D.G., "Malapert Mountain: Gateway to the Moon," Advances in Space Research, Vol. 31, No. 11, Jun. 2003, pp. 2467–2472.
26. Stooke, P.J., "Exploration Strategies and Landing Sites at the Lunar South Pole," 34th Annual Lunar and Planetary Science Conference, Mar. 2003, Abstract 1265.
27. Suntracker, Software Package, Marshall Space Flight Center Orbital Mechanics Branch, MFS–28939, Open Channel Software, 1993.

REPORT DOCUMENTATION PAGE			Form Approved OMB No. 0704-0188

1. REPORT DATE *(DD-MM-YYYY)*	2. REPORT TYPE	3. DATES COVERED *(From - To)*
01-11-2007	Technical Memorandum	

4. TITLE AND SUBTITLE
Lunar South Pole Illumination: Review, Reassessment, and Power System Implications

5a. CONTRACT NUMBER

5b. GRANT NUMBER

5c. PROGRAM ELEMENT NUMBER

6. AUTHOR(S)
Fincannon, James

5d. PROJECT NUMBER

5e. TASK NUMBER

5f. WORK UNIT NUMBER
WBS 986249.01.11.20.21.03

7. PERFORMING ORGANIZATION NAME(S) AND ADDRESS(ES)
National Aeronautics and Space Administration
John H. Glenn Research Center at Lewis Field
Cleveland, Ohio 44135-3191

8. PERFORMING ORGANIZATION REPORT NUMBER
E-16219

9. SPONSORING/MONITORING AGENCY NAME(S) AND ADDRESS(ES)
National Aeronautics and Space Administration
Washington, DC 20546-0001

10. SPONSORING/MONITORS ACRONYM(S)
NASA

11. SPONSORING/MONITORING REPORT NUMBER
NASA/TM-2007-215025; AIAA-2007-4700

12. DISTRIBUTION/AVAILABILITY STATEMENT
Unclassified-Unlimited
Subject Category: 91
Available electronically at http://gltrs.grc.nasa.gov
This publication is available from the NASA Center for AeroSpace Information, 301-621-0390

13. SUPPLEMENTARY NOTES

14. ABSTRACT
This paper reviews past analyses and research related to lunar south pole illumination and presents results of independent illumination analyses using an analytical tool and a radar digital elevation model. The analysis tool enables assessment at most locations near the lunar poles for any time and any year. Average illumination fraction, energy storage duration, solar/horizon terrain elevation profiles and illumination fraction profiles are presented for various highly illuminated sites which have been identified for manned or unmanned operations. The format of the data can be used by power system designers to develop mass optimized solar and energy storage systems. Data are presented for the worse case lunar day (a critical power planning bottleneck) as well as three lunar days during lunar south pole winter. The main site under consideration by present lunar mission planners (on the Crater Shackleton rim) is shown to have, for the worse case lunar day, a 0.71 average illumination fraction and 73 to 117 hours required for energy storage (depending on power system type). Linking other sites and including towers at either site are shown to not completely eliminate the need for energy storage.

15. SUBJECT TERMS
Lunar terrain; Energy storage; Solar energy; Radar digital elevation model; Lunar illumination; Lunar shadowing; Clementine imagery; Solar array towers; Lunar south pole; Illumination simulation; Computer program; Algorithms; Landing sites

16. SECURITY CLASSIFICATION OF:			17. LIMITATION OF ABSTRACT	18. NUMBER OF PAGES	19a. NAME OF RESPONSIBLE PERSON
a. REPORT	b. ABSTRACT	c. THIS PAGE			STI Help Desk (email:help@sti.nasa.gov)
U	U	U	UU	34	19b. TELEPHONE NUMBER *(include area code)* 301-621-0390